Synthesis and electrochromic properties of asymmetric viologen derivatives

Yerbolat Yerzhanov

Thesis Submitted in Partial Fulfillment of the Requirements for the degree of Master of Science in Chemistry at Nazarbayev University.

Astana, 2025

Supervisor: Dr. Mannix P. Balanay

ABSTRACT

Yerbolat Yerzhanov: Synthesis and electrochromic properties of asymmetric viologen derivatives

(Under the direction of Dr.Mannix Balanay)

Viologens, based on the 4,4' bipyridine scaffold, are promising functional materials due to their ability to reversibly change color under applied electrical potential. This electrochromic property makes them suitable candidates for applications in devices such as smart windows, electronic paper, and display technologies. The synthesis of asymmetric viologens provides opportunities to tailor their physicochemical properties, introduce additional functionalities, and enhance the long-term stability of both the compounds and the devices in which they are incorporated. However, the synthesis of asymmetric viologens remains a significant challenge, largely due to the electronic nature of the bipyridine core. In this study, four viologen derivatives, designated as V-COOH, V-OH, Me-V-COOMe, and Bn-V-COOH, were synthesized and employed as the active components in electrochromic devices. The compounds and resulting devices were characterized by using proton nuclear magnetic resonance spectroscopy, cyclic voltammetry, and ultraviolet-visible spectroscopy to investigate their optical behavior in both bleached and colored states. Key parameters such as maximum transmittance, optical contrast, and contrast ratio were evaluated. The results indicated that viologens with a second substituent exhibited superior electrochromic performance. Among these, Bn-V-COOH showed the lowest maximum transmittance in the colored state at 26.22 % and the highest contrast ratio of 2.26, while Me-V-COOMe demonstrated the highest optical contrast at 41.44 %. In contrast, the viologens lacking a second substituent showed markedly lower values across all optical parameters. These findings demonstrate that the presence of a second substituent is critical for optimizing the electrochromic properties of viologen-based materials.

ACKNOWLEDGEMENTS

I would like to express my deepest gratitude to my supervisor, Professor Mannix P. Balanay, for his guidance, patience, and support.

Special thanks to my senior colleague, Igor Ivanov-Pryanichnikov, for great assistance in synthesis and NMR analysis. His assistance helped break the deadlock in the synthesis process.

Thanks to Ayagoz Ibrayeva and Diana Suleimenova, who helped me design and fabricate ECDs and perform electrochemical measurements.

I would also like to thanks all my colleagues, committee members, friends, and others who contributed to and supported my work.

TABLE OF CONTENTS

LIST OF TABLES

LIST OF FIGURES

LIST OF ABBREVIATIONS

AP – 4-aminophenol

Bipm – bipyridine

Bn-V-COOH – [1-(benzyl)-1′-(4-carboxyphenyl)-(4,4′-bipyridinium)]$^{2+}$

CV – cyclic voltammetry

DNCB – 2,4-dinitrochlorobenzene

DNP-V-COOH – [1-(2,4-dinitrophenyl)-1′-(4-carboxyphenyl)-(4,4′-bipyridinium)]$^{2+}$ dichloride

DNP-V-OH – [1-(2,4-dinitrophenyl)-1′-(4-phenoxy)-(4,4′-bipyridinium)]$^{2+}$ dichloride

ECD – electrochromic device

EtAc – ethyl acetate

FTO – fluorine-doped tin oxide-coated glass

ITO – indium-tin oxide-coated glass

Hx – hexane

Me-V-COOH – [1-methyl-1′-(4-carboxyphenyl)-(4,4′-bipyridinium)]$^{2+}$ iodide/chloride

V-COOH – [1-(4-carboxyphenyl)-(4,4′-bipyridinium)]$^{+}$ chloride

V-DNP – [1-(2,4-dinitrophenyl)-(4,4′-bipyridinium)]$^{+}$ chloride

V-OH – [1-(4-phenoxy)-(4,4′-bipyridinium)]$^{+}$ chloride

PABA – 4-aminobenzoic acid

PC – propylene carbonate

PMMA – poly(methyl methacrylate)

1. INTRODUCTION

1.1 Background

The electrochromic properties of viologens (derivatives of 4,4'-bipyridine) are characterized by forming differently colored oxidation states under applied voltage (Figure 1). Among electrochromes, viologens are distinguished by their desirable electron-accepting capability, the stability of bipyridinium radical (one of the most stable known organic radicals [1]), and high modification potential. These qualities made viologens one of the most extensively studied electrochromic materials, which found application in manufacturing electrochromic display devices, memory devices, molecular machines, antibacterial agents, electrodes for supercapacitors and batteries, catalysts for hydrogen generation, etc. [2-6].

Figure 1. Electrochromic properties of dimethyl viologen.

The electrochromic properties of viologens were first investigated in 1973 (Figure 2), but in recent years, viologen-based electrochromic devices have been actively commercialized. In 2003, NTera Ltd. developed a representative viologen-based EC display called NanoChromics. They cleverly used anchoring viologen on the surface of mesoporous TiO_2 and used Sb-doped SnO_2 as the counter electrode material.

Then, several viologen derivatives with different substituents were used for multicolors, demonstrating high durability and good cyclic life (approximately 50,000 cycles). To date, the most widely known commercial ECDs are dimmable windows installed on the Boeing 787 Dreamliner [2]. EC smart windows have been applied to the windows of cars and buildings, and gradually, EC materials are expanding into portable consumer electronics.

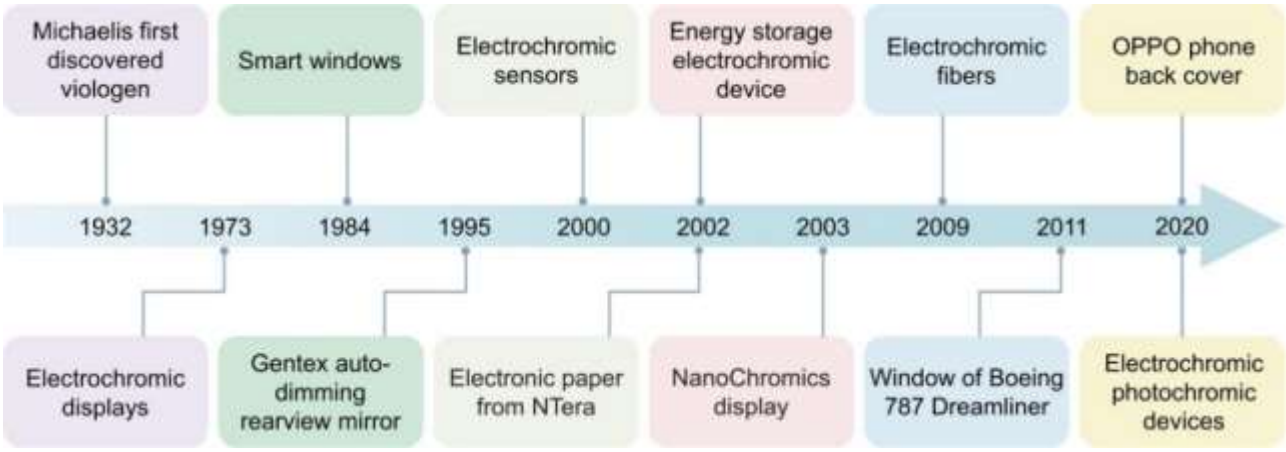

Figure 2. The brief history of viologens. Adapted with permission from ref.3. Copyright 2024 Science Press and Dalian Institute of Chemical Physics, Chinese Academy of Sciences. Elsevier and Science Press.

Multiple reviews have been dedicated to the synthesis and application of viologens in different areas: general synthesis [4], organic batteries [5], flexible devices [3,6], and electrochromic devices [7].

1.2 Ageing and dimerization

After prolonged cycling between the colored and bleached states, viologen-based ECD forms an unsightly yellow–brown stain on the electrode, a dimerized radical-cation [7]. In the best case, the formation of the radical-cation dimer is quasi-reversible, and oxidation at an electrode is slow within a realistic timescale; hence, in that way, ECDs containing traces of the dimer soon will fail. The dimerization is a common problem in viologen redox chemistry: its fast rate constant and moderate equilibrium constant make comproportionation inevitable whenever neutral species are formed at an electrode. To inhibit the dimerization of viologen radical cations, the following

approaches were proposed: (i) using asymmetric ECMs, (ii) using stronger electrostatic repulsion groups (e.g.; trifluoromethyl group), and (iii) using bulkier groups to avoid the contact chance of viologen radical cations (e.g, triphenylamine) [8].

1.3 Modification of viologens

Multiple strategies have been suggested to synthesize novel viologen-based functional materials with improved properties. The most popular modifications and approaches are discussed in this section.

N-alkylated viologens – the most straightforward approach: the reaction between halogenated alkanes and 4,4'-bipyridine is a common, convenient, and high-yield method to prepare alkyl N-substituted viologens directly. This method is the earliest discovered one and has a wide application. The N-alkylated viologens can be obtained via quaternization reaction with the corresponding halogenide. The viologen's properties can be easily modulated by replacing the substituted alkyl chain (length of the alkyl chain or the peripheral ending group) or by altering the counter anion category (Figure 3). The color of the radical cation tends towards crimson as the length of the alkyl chain increases, mainly owing to the increasing incidence of radical-cation dimerization; the dimer of alkyl-substituted radical cations is red.

N-arylated viologens – aryl-substitution conjugation allows the production of green or dark-red radical-cation salts (e.g.; Ph-CN produces green [7]). The direct arylation of viologens with halogenated aryls is impossible. Therefore, the common approach is to synthesize via the Zincke reaction. A more detailed explanation of the mechanism of the Zincke reaction is discussed further.

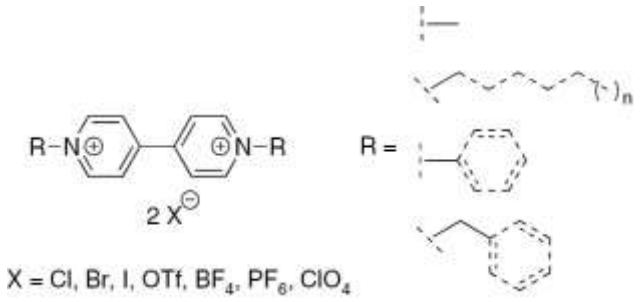

Figure 3. The N-substituted viologens.

N-fused viologens – an aromatic extension of the p-system of viologens through forming a bridge at 2,2’ and/or 5,5’ positions, allowing modulation of the electron affinity of a molecule. Fused viologens can be divided into two types according to the bridging between two QPSs: heterocyclic ring and benzene- or acene ring-fused viologens (Figure 4) [1].

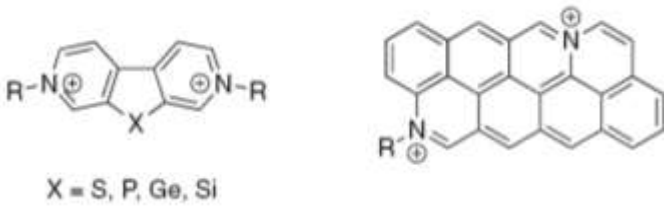

Figure 4. The fused viologens: heterocyclic (on the left) and acene ring fused (on the right).

Extended viologens – introducing spacers (Figure 6) in viologen can greatly enhance the scope of electronic and photophysical properties while still maintaining the stable redox behavior of the viologen system and its potential applications as an electrochromic. Further modification of N-fused viologens is not so often used; however, some works for asymmetric phosphoryl-bridged viologen have been published [3].

Figure 5. The extended viologens.

Polyviologens – immobilization of viologen in polymeric structures improves stability, mechanical properties, and solvent processability of electrochrome. Viologen polymers can be divided into (i) the position of the viologen – the main backbone or side chain (Figure 6), (ii) the presence or absence of conjugation, and (iii) linear and cross-linking.

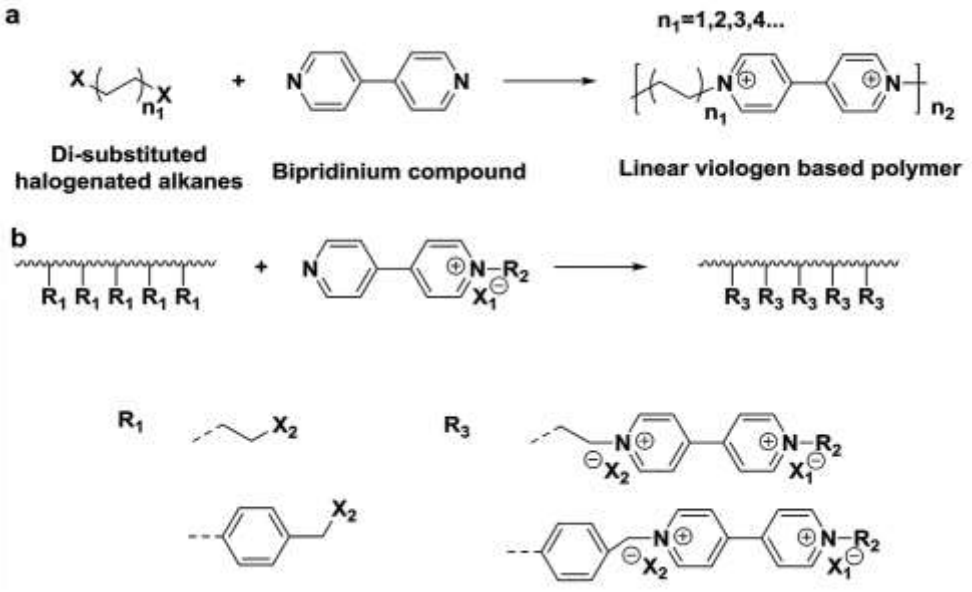

Figure 6. Polyviologens: (a) in main-chain, (b) in side-chain.

Organic frameworks — viologens can be linkers inside metal-organic and covalent organic frameworks (MOF and COF, respectively). Viologen-based MOFs and COFs are prepared via previously mentioned N-alkylation and Zincke reactions with triple functional species (such as 1,3,5-Tris(bromomethyl)benzene and melamine) [9]. The example of COF is shown in Figure 7.

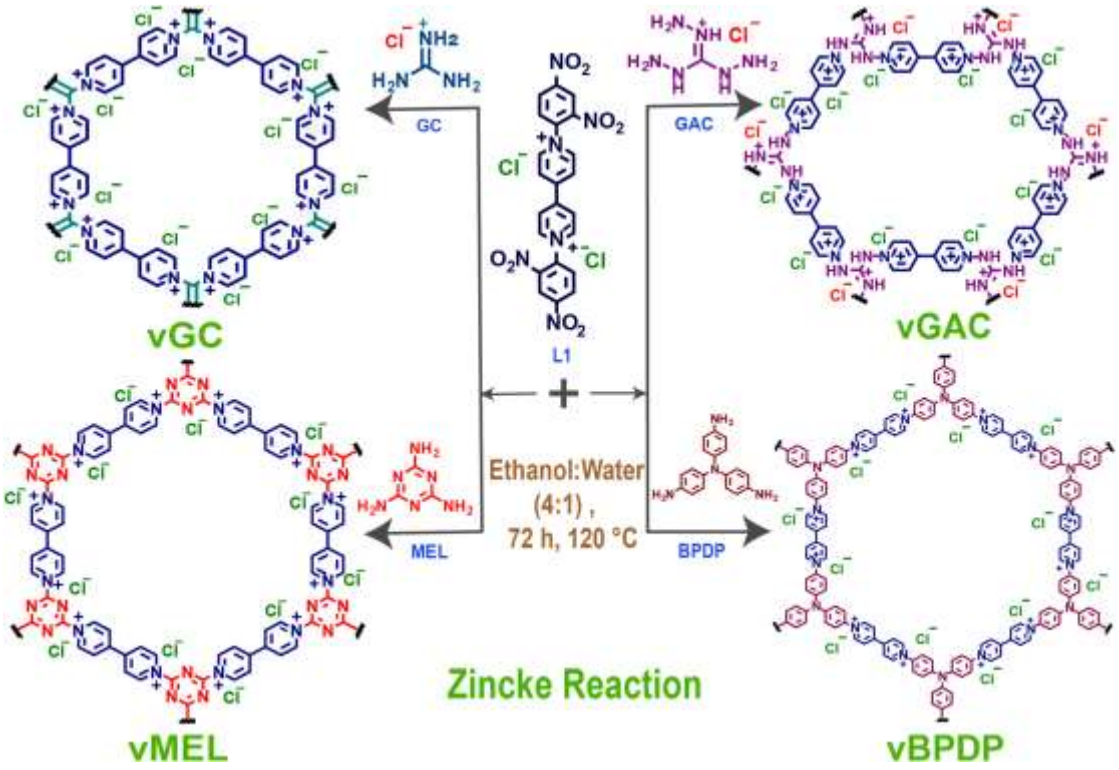

Figure 7. Viologen-based COFs [9].

1.4 Zincke reaction mechanism

Zincke reaction consists of two steps shown in Figure 8: (1) addition of dinitrophenyl group (DNP) via nucleophilic aromatic substitution (SnAr), (2) substitution of dinitrophenyl group (DNP) with aryl group via ANRORC (addition of Nucleophile, Ring-Opening, Ring-Closing) mechanism [11].

Figure 8. The Zincke reaction overview.

1.4.1 Addition of Nucleophile

Generally, direct arylation of pyridine's nitrogen is unfavorable because of the nucleophilicity of both reagents; however, the two nitro groups of DNCB provide enough electro-withdrawing effect to make the reaction possible. The SnAr proceeds in two steps, which are shown in Figure 9. In the case of bipyridine, the electron-withdrawing effect of the second pyridine ring decreases the nucleophilicity of the electron pair, decreasing the reactivity of each separate nitrogen.

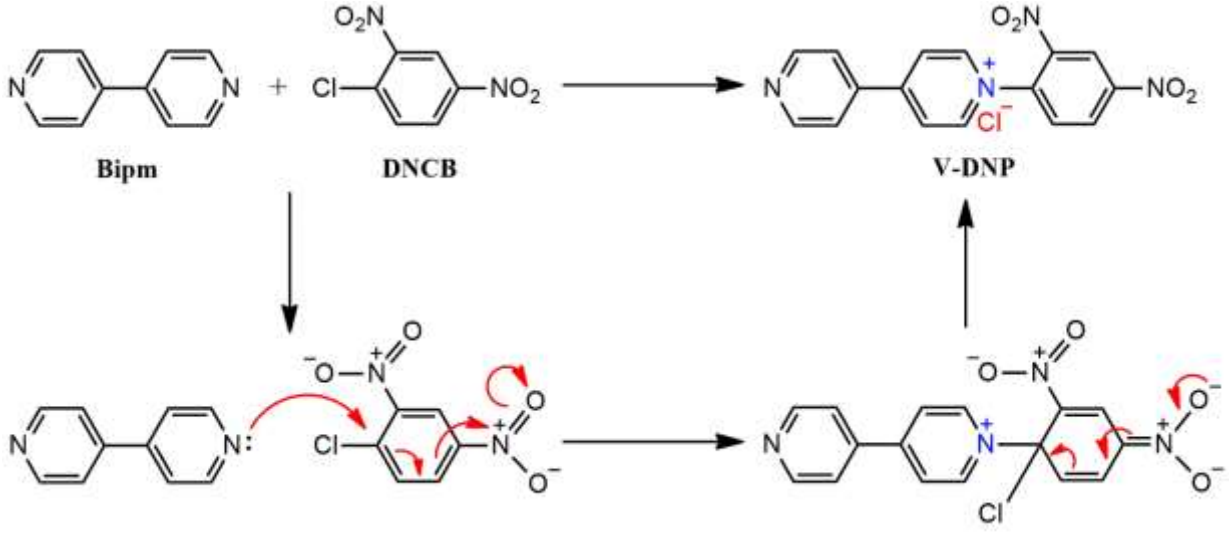

Figure 9. The nucleophilic addition of DNCB to pyridine.

Zincke reaction proceeds better with alkyl amines and initially was used for regioselective synthesis [9]. The kinetics of the Zincke reaction for simple pyridine using conventional and microwave irradiation was studied by Zeghbib et al. in 2016 (Figure 10) [10]. In their works, they found the pKa dependence of aniline substitution: aniline derivatives with pKa less than 2.5 demonstrated low (less than 20%) yields at conventional heating at 80 °C for 96 h, 0.2 mmol of N-(2,4-dinitrophenyl)-pyridinium chloride, with two equivalents of aniline derivative ($RC_6H_4NH_2$) in mixture EtOH/H_2O: 60/40 (1mL). Other methods of arylation of pyridine exist but are less popular due to the lower versatility.

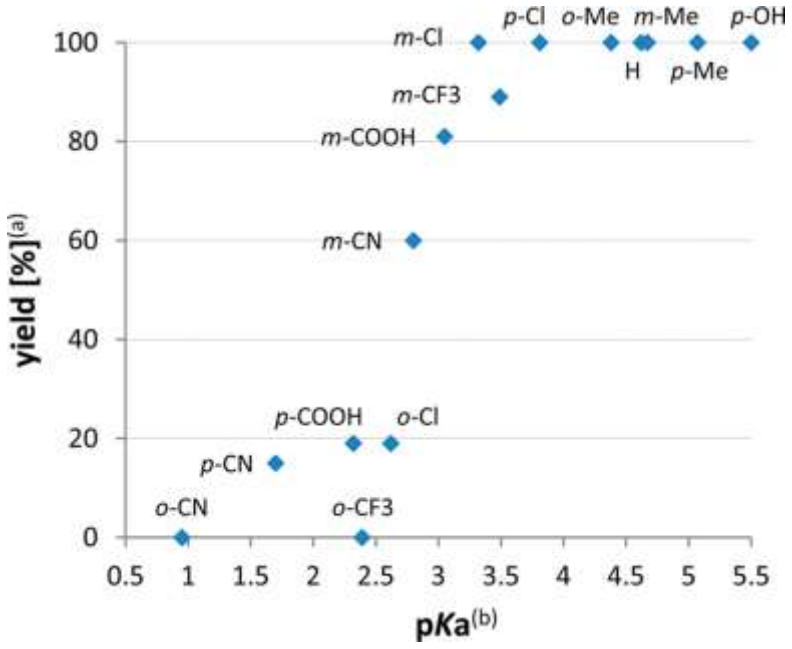

Figure 10. The reactivity of different aniline derivatives. Adapted with permission from ref. 10. Copyright 2016, American Chemical Society.

1.4.2 Addition Nucleophile, Ring-Opening, Ring-Closing

The possible mechanism is presented in Figure 11 [11]. In case of bipyridine, the electron-withdrawing effect of the second pyridine ring should positively affect the formation of Zincke salt, accelerating the ring opening. Similarly, the aniline derivatives with electron-donating groups also positively affect the reaction, which will be discussed later in this part. Lastly, the addition of Et_3N positively affects the Zincke reaction, particularly by facilitating the six-step process (deprotonation with formation of imine, step **6** in Figure 11) [11].

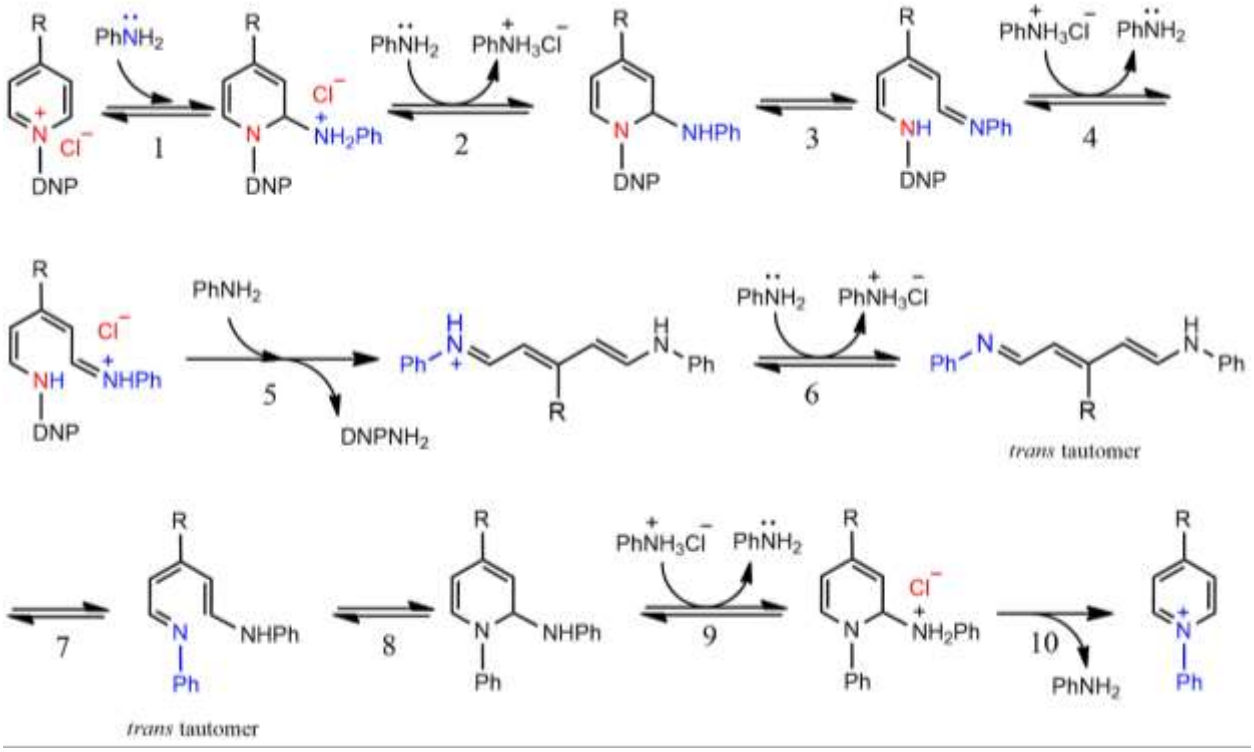

Figure 11. The mechanism of aryl-substitution of the Zincke salt [11].

1.5. Highlights of recent contributions

The library of viologens is actively expanding: novel viologen-based materials are synthesized and investigated. This part mainly focuses on works dedicated to electrochromic asymmetric viologens, mentioning some distinguished works in cross-disciplinary fields.

1.5.1 Multichromism

Achieving a broad palette of colors is crucial for practical application, yet most studies have only shown single-color changes or created devices that display a single pattern. Some methods to develop multicolor ECDs include integrating multiple electrochromic materials. However, because these materials often share similar redox potentials, their color changes tend to overlap, leading to unclear color states. To address this, strategies that allow for the independent control of each chromophore's coloration are needed.

Choi et al. 2022 prepared multicolor, dual-image, printed electrochromic displays (ECDs) obtaining five diverse colors (e.g.; cyan, green, magenta, emerald, and yellow shown in Figure 12) by the addition of different electron-withdrawing groups. Their devices show fast switching speed ($t_c \sim 2.0$ s, $t_b \sim 1.5$ s), and high coloration efficiency (avg. ~ 328.8 cm2/C), which is attributed to the large surface area of the hybrid electrode [12]. Researchers tested "tandem configuration" – they inserted a double-sided fluorine-doped tin oxide electrode (dsFTO) between two hybrid electrodes, making dsFTO serve as a counter electrode of both hybrid electrodes, allowing independent or simultaneous operation of each hybrid electrode through adjusting the applied voltage. The different coloration was achieved by asymmetric functionalized of various phosphonated viologens, applied on mesoporous titanium dioxide (TiO_2) presented in Figure 13.

Figure 12. The multicolored ECDs. Adapted with permission from ref.12. Copyright 2021 Elsevier.

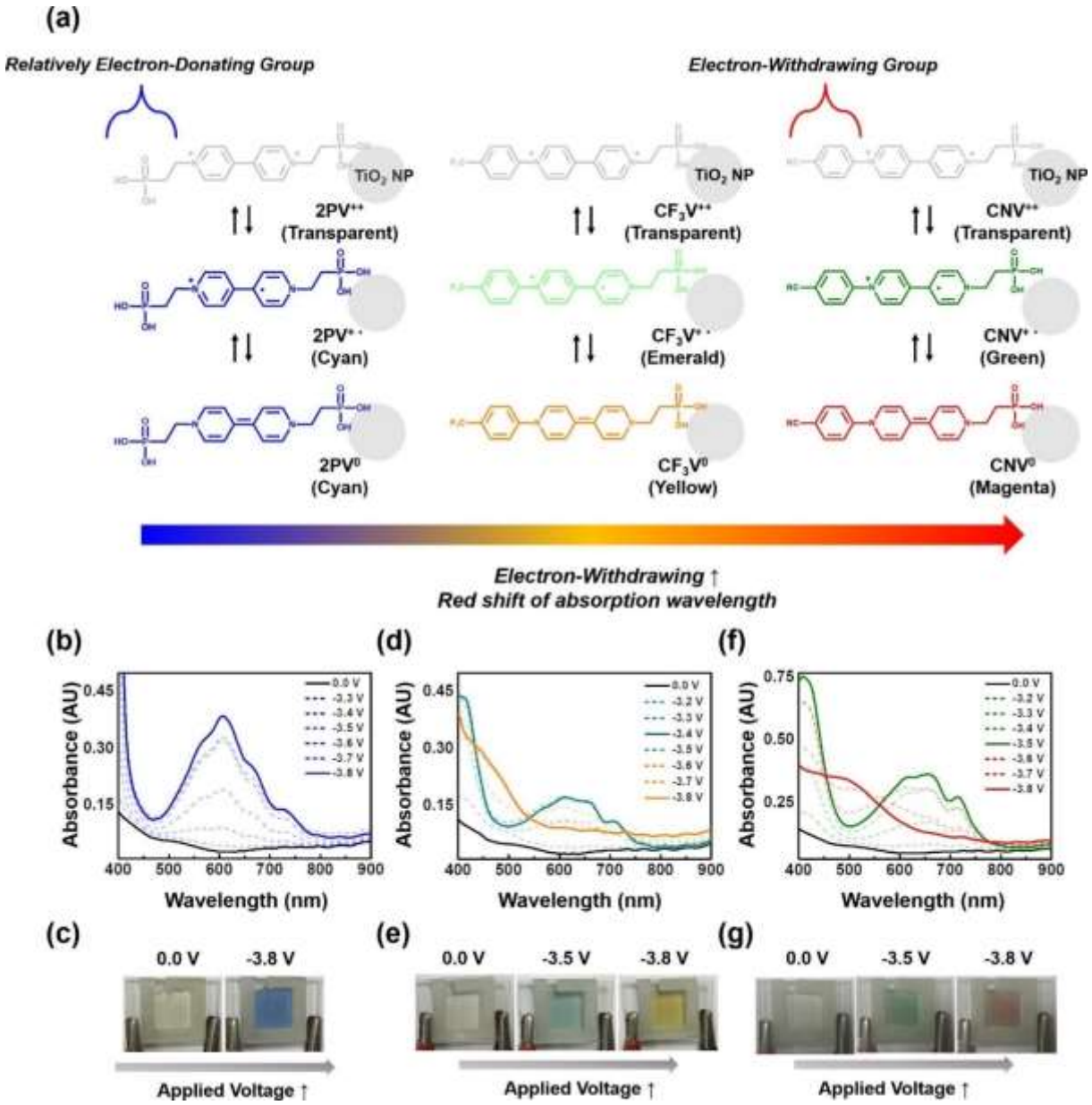

Figure 13. The various phosphonated viologens. Adapted with permission from ref. 12. Copyright 2021 Elsevier.

1.5.2 Electrolytic gels

Electrolytic gels are an effective strategy for immobilizing viologens. The previously mentioned dimmable windows on the Boeing 787 Dreamliner have been developed and patented by the Gentex company and consist of electrochromic gel [13]. Alesanco et al synthesized two

asymmetrical viologens (1-ethyl-1′-(*p*-cyanophenyl)-4,4′-bipyridinium dibromide (Et-pCNVio) and 1-benzyl-1′-(*p*-cyanophenyl)-4,4′-bipyridinium dibromide (Bn-pCNVio) and impregnated them in PVA-borax electrolytic matrix according to the procedure shown in Figure 14. Additionally, three symmetrical (pCNVio, EtVio, and BnVio) had been synthesized to compare performance characteristics of gels containing asymmetric viologens and a blend of two symmetric components [14].

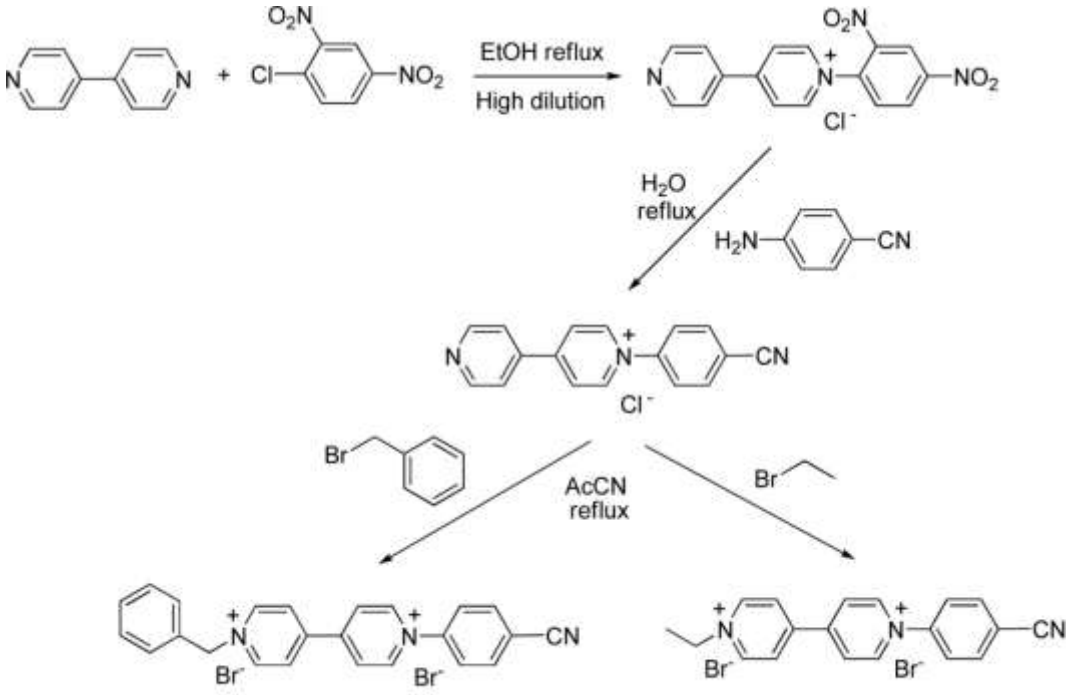

Figure 14. The synthetic routes for Et-pCNVio and Bn-pCNVio. Adapted with permission from ref. 14. Copyright 2016 American Chemical Society.

Kim et al prepared 1-benzyl-1′-heptyl viologens and found that such asymmetric molecular structures attribute to the suppression of dimer production when used as EC chromophores. ΔT was maintained at ~82% of ΔT_o after continuous operation for 30,000 s compared to 54% of BHV^{2+}[15] Based on ECDs than DHV^{2+}-based ECDs, as well as the importance and effectiveness of molecular tuning of EC chromophores [15]. The shortest coloration time e (t_c=10.6s) was achieved at -1.2 V, which is slower than DHV^{2+}-(t_c=5s). Compared with other electrochromic systems, the suggested system has modest speed but superior stability compared to other electrochromic systems presented in Table 1 [16].

Table 1. The comparison of different electrochromic systems. Adapted with permission from ref. 16. Copyright 2023 Elsevier.

`EC	Electrolyte	i_{max} (nm)	t_b (s)	t_c (s)	ΔT (%)	CE (cm^2C^{-1})	Stability (cycles)
WO_3	H_2SO_4	632	3	5	89	51.1	1000
WO_3	$Al(ClO_4)_3$+PC	633	12	12	87	105	1500
WO_3	$LiClO_4$+PC	630	6.0	11.5	81.7	57.71	100
Aniline derivatives	$LiClO_4$+PC	720	4.2	0.8	70	328.5	1000
Prussian blue	LITFSI + PC	680	26	17	59.94	73.5	10000
NiO	KOH	550	1.55	2.11	78.20	11.20	100
Viologens	$[BMIM][BF_4]^+$ dmFc	605	29	10.6	42	123.4	30000
Viologens	PVA + LiCl	550	1.2	2.8	40	989	200
Viologens	PVA + borax	600	7	14	60	-	15000
Viologens	$TBAPF_6$	610	5.9	2.6	55.8	125.1	3000

1.5.3 Flexible devices

Flexible ECDs are another promising direction in the development of viologen-based EC. The key to developing stable EC films is firmly adhering to flexible substrates. Qian et al synthesized two symmetric viologen derivatives of 1,1′-bis(4- (dimethylamino) phenyl)-[4,4′-bipyridine] dihexafluorophosphate (DNPV) and 1,1′-bis(4-acetamidophenyl)-[4,4′-bipyridine] dihexafluorophosphate (DAcPV) and two asymmetric viologen derivatives of 1- benzyl-1’-(4-(dimethylamino)phenyl)-[4,4′-bipyridine]dihexafluoro- phosphate (Bn-NPV) and 1-(4-acetamidophenyl)-1′-benzyl-[4,4′-bipyridine]dihexa-fluorophosphate (Bn-AcPV) shown on Figure 15 [17].

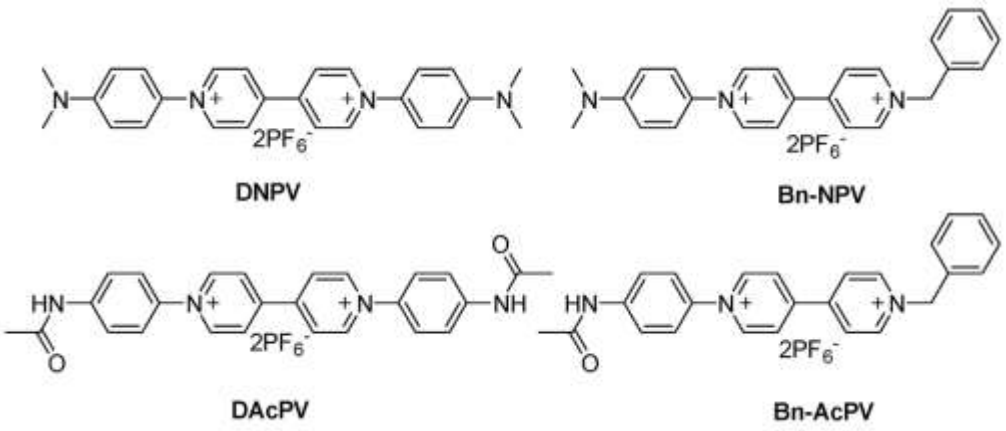

Figure 15. The asymmetric viologens for flexible ECDs. Adapted with permission from ref. 17. Copyright 2023 Elsevier.

The obtained solution was tested using a flexible bending tester to repeatedly bend the flexible device at a bending radius of 1.12 cm. The UV–vis spectra of the flexible ECDs were measured after the bending test (Figure 16). After 1000 bending cycles, the optical contrast retentions of flexible ECDs based on DNPV, Bn-NPV, DAcPV, and Bn-AcPV were 98 % (731 nm), 63.6 % (665 nm), 83 % (574 nm), and 99 % (611 nm), respectively. The results show that the prepared flexible devices have good bending properties (Table 2).

Table 2. The characteristics of flexible and rigid ECDs. Adapted with permission from ref. 17. Copyright 2023 Elsevier.

ECD	ΔT(%)	t_c/t_b (s)	Coloration efficiency (cm^2/C)	Cycle stability after 1000 cycles (%)
DNPV(flexible)	33.4	15.8/25.0	84.83	72.1
Bn-NPV(flexible)	49.5	15.5/27.2	143.68	72.6
DAcPV(flexible)	80.4	27.5/133.0	286.95	86.3
Bn-AcPV(flexible)	66.6	15.5/44.7	203.95	96.0
DNPV(rigid)	38.0	11.7/36.3	157.07	80.4
Bn-NPV(rigid)	34.1	14.0/20.5	110.88	81.4
DAcPV(rigid)	87.1	20.5/92.2	435.58	70.6
Bn-AcPV(rigid)	60.0	12.2/21.0	113.80	92.8

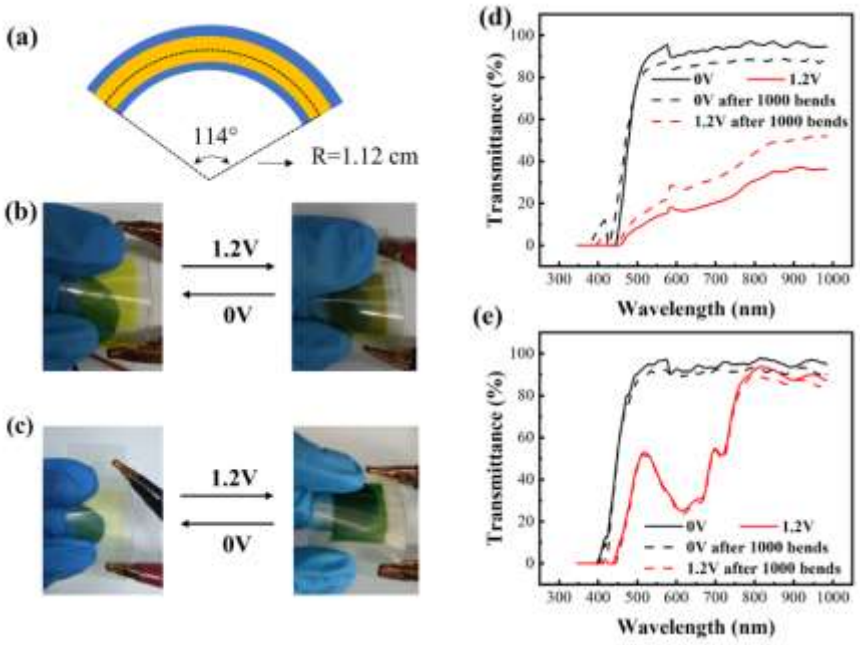

Figure 16. The evaluation of flexible ECDs. (a) Schematic diagram of the flexible ECDs bending test. Images of reversible color switching of the ECD based on (b) DAcPV and (c) Bn-AcPV. The UV–vis spectra of the ECD based on (e) DAcPV and (f) Bn-AcPV under different applied voltages before and after 1000 bends. Adapted with permission from ref. 17. Copyright 2023 Elsevier.

1.5.4 Microwave-assisted synthesis

Microwave irradiation is applied to improve yield and accelerate the procedure. Several papers were published in an attempt to optimize the synthesis of symmetric and asymmetric viologens, bis-viologens, polyviologens, and viologen dendrimer structures [18].

Komoda et al. 2021 prepared viologen nanoparticles via a microwave heating technique. This work is distinguished by investigating the microwave kinetics of short alkyl substituent (EtBr) and benzyl substituent (BnBr). They proceeded with the reaction with a reagent ratio [BPy]/[R-Br]=1:3 in DMF (Bipm 1.3 mmol, DMF 10 mL). Interestingly, the benzyl substituent's conversion is much higher than alkyl: comparing conversion and reaction yield after 10 minutes at 80°C, the benzyl substituent converted 81%, while ethyl bromide only 6%. The 10-minute reaction at 150 °C results in 53% conversion of EtBr. To improve reaction conversion, they increase the amount of EtBr by 10 times (achieving the ratio [Bipm]/[R-Br]=1:30) and get 24% conversion after 10 minutes at 80°C, obtaining only the mono-substituted component.

They exploited this investigation to control the growth of the viologen nanoparticles, using 1,3,5 tris (bromomethyl)benzene (TBMB) as the branching agent and EtBr as the termination agent: At the first stage, the reaction proceeds at 80°C to provide the chain propagation, then it terminated with rising temperature up to 150°C t (Figure 17). The nanoparticle diameter was determined to be 142±15nm for the first stage reaction time of 10min, which increased to 269±67nm at 20min, as evidenced by dynamic light scattering measurements.

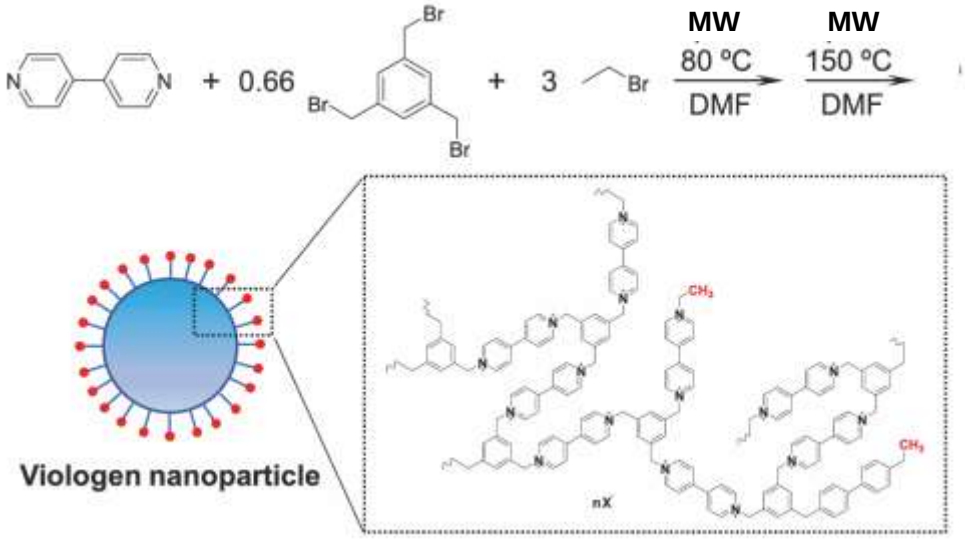

Figure 17. One-pot synthesis of viologen nanoparticles by microwave heating. Adapted with permission from ref. 18. Copyright 2021, under exclusive licence to The Society of Polymer Science, Japan.

1.5.5 Molecular machines

Viologens are widely used in the preparation of molecular machines. The supramolecular complexation of viologens into crown ethers, cyclodextrins, and cucurbiturils (CB[7] and CB[8]) host molecules has been recently studied, including the preparation of photochromic materials. The host-guest interactions are highly sensitive to the *N*-substituents of the viologens.

Chen et al demonstrated the first synthesis of viologen-quinoid conjugates using the facile nucleophilic N-substitution reaction between pyridyl nitrogen and an AQM ditriflate. The iAQM viologens showed strong electron-accepting properties, reversible redox properties, and visible

absorption features, combining characteristics of both the viologen and quinoid units. Computational calculations have been performed using the TD-DFT method using a 6-31G* basis set. According to calculations, it is possible to construct narrow bandgap donor-acceptor polymers based on the iAQM viologen unit, with a predicted optical bandgap below 1 eV [19].

1.6 Design of asymmetric viologens

The rich library of viologen materials and ECDs continuously expands, and new structures and solutions have been synthesized and published. The literature analysis showed two promising areas, which are mainly overlooked but have huge research potential: asymmetric design and conducting polymer.

Asymmetric strategy – despite the fact, that the majority of studies mainly focused on the synthesis and application of symmetric viologen, rather than asymmetric ones, the alternating of viologen symmetry is a promising approach: (i) asymmetry suppresses dimerization, which increases the stability of ECDs [7]; (ii) better control on electrochromic performance – the structure of asymmetric viologen could be designed according to donor-accepting approach; (iii) functionalization of viologens, particularly creation of anchoring side.

The aim of the research is to develop asymmetric viologen-based electrochromic materials. Four structures with different functional groups have been proposed and shown in Figure 18.

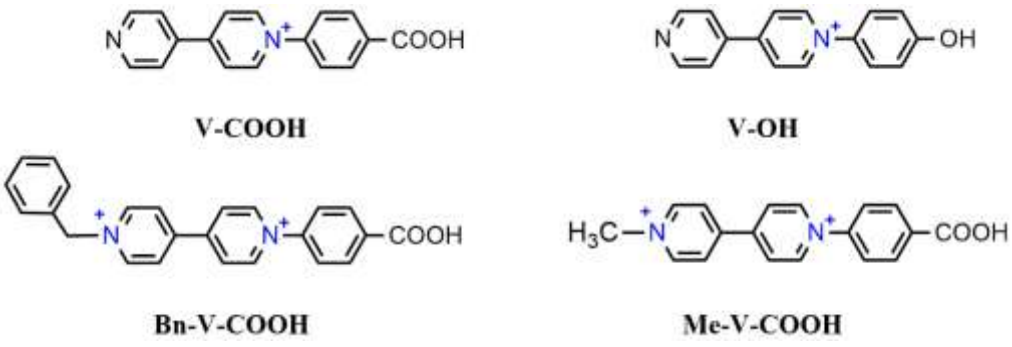

Figure 18. The proposed viologen structures.

- V-COOH – [1-(4-carboxyphenyl)-(4,4′-bipyridinium)]$^{+}$ chloride – carboxyphenyl group creates conjugation, red shifting color of compound, and additionally, the carboxyl moiety plays the role of an anchor for the application of viologen onto the TiO_2 surface.
- V-OH – [1-(4-phenoxy)-(4,4′-bipyridinium)]$^{+}$ chloride – phenoxy group is an electron-donating group, which should positively work with electron-deficient bipyridine.
- Me-V-COOH – [1-methyl-1′-(4-carboxyphenyl)-(4,4′-bipyridinium)]$^{2+}$ iodide/chloride – small methyl group allows for maximizing the polarity of the molecule, making it more soluble in water.
- Bn-V-COOH – [1-benzyl-1′-(4-carboxyphenyl)-(4,4′-bipyridinium)]$^{2+}$ bromide/chloride – benzyl group decreases the polarity of the molecule, making it more soluble in organic solvents.

The proposed structures were used as the base for ECDs and were characterized via physico-chemical methods, including ^{1}H-NMR spectroscopy, cyclic voltammetry (CV), UV-Vis spectroscopy, etc.

2. MATERIALS AND METHODS

The synthesis plan (Appendix A) was designed with great emphasis on the assistance of a microwave reactor to accelerate reactions from 70-90 hours to a few hours [20]. The main starting reagent is 4,4'- bipyridine, which was activated for nucleophilic substitution via Zincke reaction with 2,4-dinitrochlorobenzene (DNCB) and then modified with different aniline derivatives. DNCB has been synthesized by nitration of chlorobenzene with concentrated nitric acid (>65%) in the presence of sulfuric acid (>95%). Aniline derivatives include 4-aminobenzoic acid, 4-nitroaniline, and 4-aminophenol.

The analysis of the obtained viologen derivatives structures was proceeded using ^{1}H-NMR in DMSO-d_6. The electrochromic properties of dissolved and applied viologens were analyzed by cyclic voltammetry (CV), UV-Vis spectroscopy in tandem with chronoamperometry.

2.1 Reagents

The main starting reagent is 4,4'- bipyridine, is activated for nucleophilic substitution via Zincke reaction with 2,4-dinitrochlorobenzene (DNCB) and then modified with different aniline derivatives. DNCB has been synthesized by nitration of chlorobenzene with concentrated nitric acid (conc.>65%) in the presence of sulfuric acid (conc.>95%). Aniline derivatives include 4-aminobenzoic acid and 4-aminophenol.

The materials of electrolytes include poly(methyl methacrylate) (PMMA), propylene carbonate (PC), lithium perchlorate ($LiClO_4$), and ferrocene (Fc). The fluorine-doped tin oxide-coated glass (FTO) pieces were used as a base for ECDs and substrate for further layers. The NMR spectrum was recorded on Jeol JNM-ECA500.

2.2 Synthesis of viologen derivatives

2.2.1 Synthesis of DNCB

DNCB was synthesized by two-step nitration of chlorobenzene in one pot (Figure 19). The ratio of Chlorobenzene:HNO3:H2SO4 was 1:5:5. The structure of DNCB was analyzed by 1H-NMR (Figure 20). The obtained DNCB was used in further reaction with bipyridine

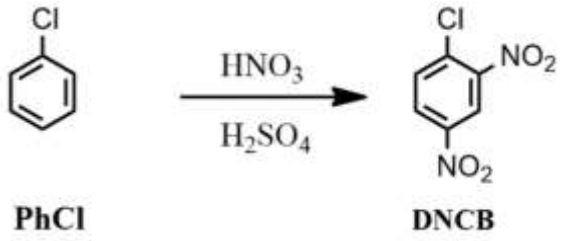

Figure 19. The synthesis of 2,4-dinitrochlorobenzene.

Pure DNCB was obtained after two recrystallisations in ethanol. The 1H-NMR (500 MHz) spectrum of 2,4-dinitrochlorobenzene (DNCB) in CDCl3 δ 8.74 (t, J = 2.9 Hz, 1H), 8.40 (dd, J = 8.8, 2.6 Hz, 1H), and 7.82 (dd, *J* = 8.8, 1.2 Hz, 1H).

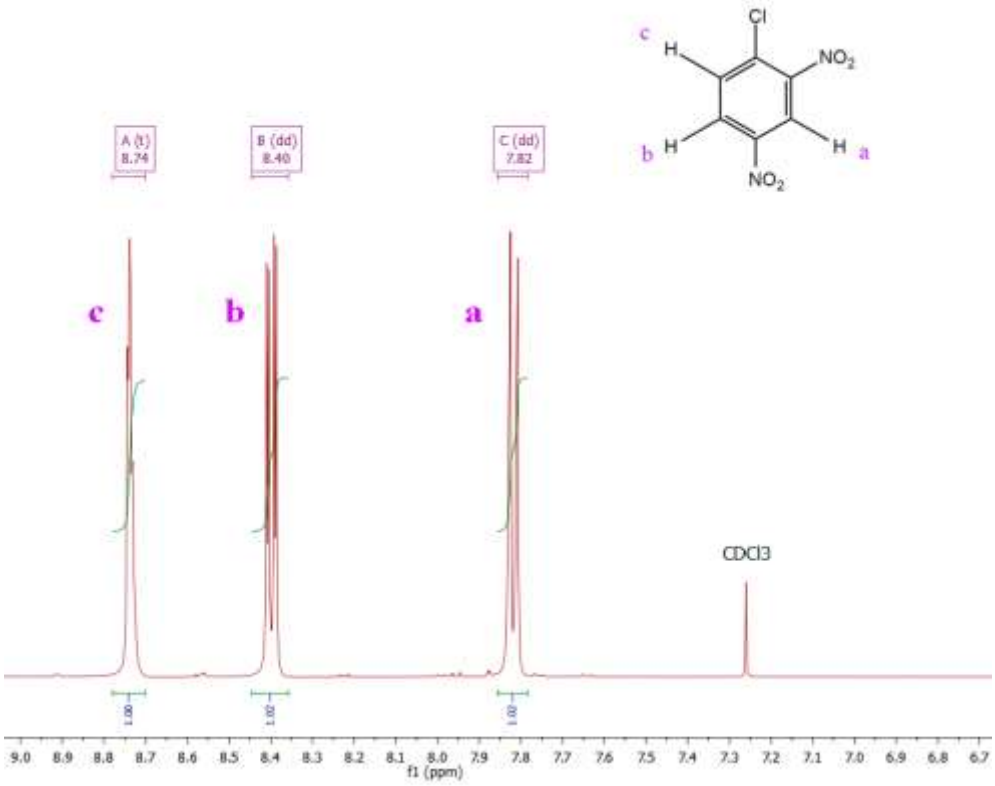

Figure 20. The ^{1}H-NMR spectrum of DNCB in $CDCl_3$.

2.2.2 Synthesis of V-DNP

The mono-substituted Zincke salt of bipyridine (V-DNP) was synthesized by reaction between bipyridine (Bipm) and DNCB in a polar solvent (typically EtOH) in MW conditions at 80-100°C (Figure 21). The reaction progress was monitored by TLC, using Hx: EtAc=1.0:1.0 and pure methanol system until the full conversion of DNCB, which is usually used in deficiency. After reaction completion, the solvent was evaporated, then V-DNP was precipitated by adding EtAc and centrifuged. The obtained product was washed three times with EtAc and then dried in a vacuum at room temperature.

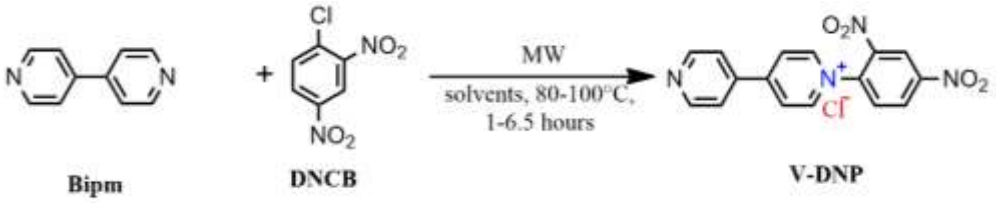

Figure 21. The scheme of synthesis of V-DNP.

Table 3. The optimization protocols for the synthesis of V-DNP.

	Bipm (mg)	DNCB (mg)	Ratio	Solvent (ml)	Temp. (°C)	Time (hours)	Prod. (mg)	Yield (%)
1	405	313	1.7:1.0	10 mL 80% EtOH	85	6.5 hours	377	68
2	121	93	1.7:1.0	3 mL 80% EtOH	100	3 hours	142	86
3	94	121	1.0:1.0	3 mL of 96% EtOH	100	3 hours	55	26
4	162	125	1.7:1.0	3 mL of dioxane	100	-	-	-
5	202	156	1.7:1.0	3 mL of acetone	100	5 hours	31	-
6	94	122	1.0:1.0	3 mL ethylene glycol	100	5 hours	-	-
7	94	122	1.0:1.0	3 mL 80% EtOH	100	3 hours	97	11
8	188	243	1.0:1.0	3 mL 80% EtOH	100	3 hours	222	0
9	93	122	1.0:1.0	3 mL tert BuOH (2 hours) + 0.6 mL H_2O (add. 2 hours)	100	4 hours	117	45
10	94	121	1.0:1.0	3 mL 60% EtOH	100	3 hours 10 min.	88	52
11	94	121	1.0:1.0	3 mL H_2O	100	1 hour 10 min	117	55
12	94	122	1.0:1.0	3 mL of 60% EtOH	80	3 hours 10 min	69	41
13	141	122	1.5:1.0	3 mL of 60% EtOH	80	2 hours 10 min.	163	55
14	104	121	1.1:1.0	3 mL of 60% EtOH	80	3.5 hours	155	-
15	94	121	1.0:1.0	3 mL of 60% EtOH in a pressure tube. oil bath	80	>2 days	-	-
16	1002	121	1.1:1.0	10 mL of 60% EtOH	80	3.5 hours	143	69

All reaction protocols are presented in Table 3. Reaction 1 has been performed in the MCR-3SX microwave chemical reactor. Different solvent systems have been tested, including EtOH (96%, 80%, 60%), water, acetone, tert-BuOH, dioxane, and ethylene glycol. The dioxane showed terrible stability in MW, while ethylene glycol, vice versa, showed good performance in MW, but the product could not be separated from the solvent due to high viscosity. Generally, a 60% solution of ethanol showed good stability in MW, good yield, and was relatively easy to separate. Reaction 15 proceeded in a pressure tube without MW irradiation; the first visible spot on TLC was observed only after 2 days, but the procedure was not carried out until the end.

The ^{1}H-NMR (600 MHz, DMSO-d_6) of V-DNP: δ 9.58 (d, J = 6.4 Hz, 2H), 9.15 (d, J = 2.5 Hz, 1H), 9.01 (dd, J = 8.7, 2.3 Hz, 1H), 8.98 – 8.91 (m, 2H), 8.46 (d, J = 8.7 Hz, 0H), 8.20 (d, J = 5.5 Hz, 1H). Yield 67%. The common impurities are unreacted bipyridine and disubstituted Zincke salt (DNP-V-DNP).

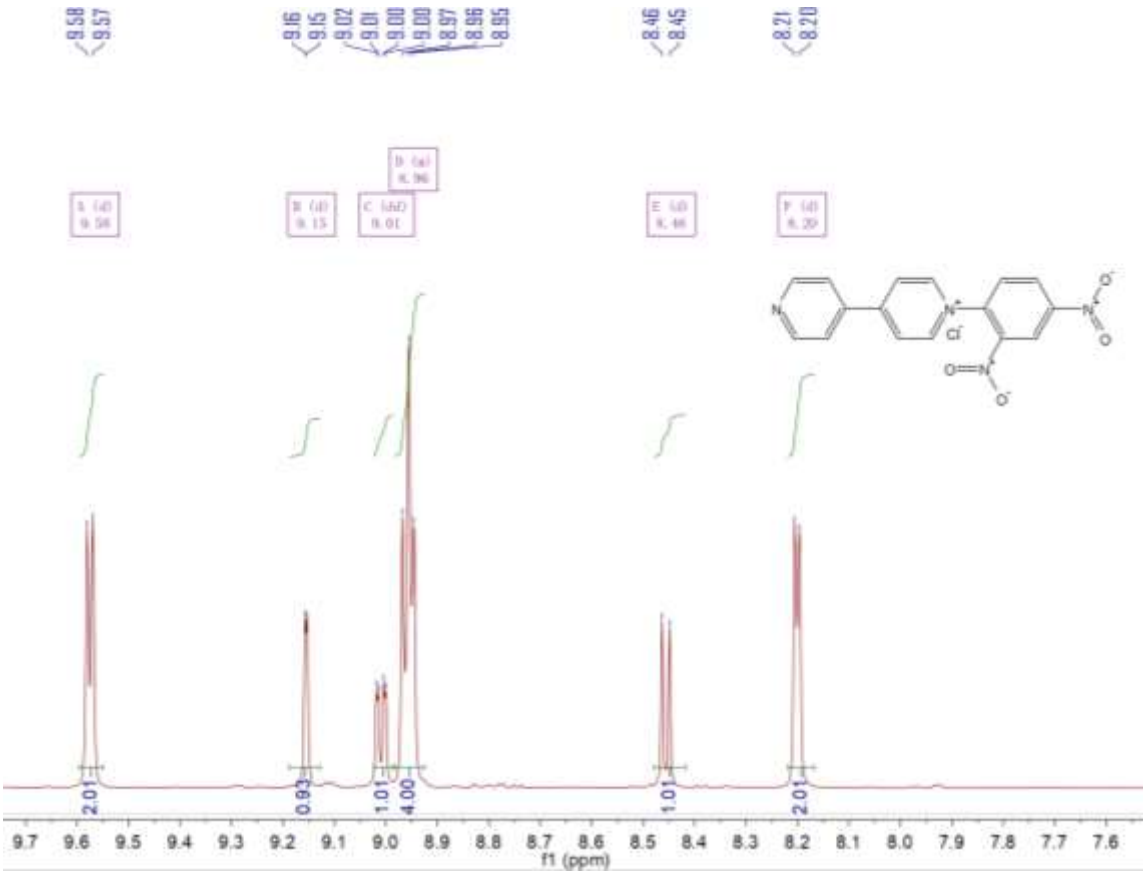

Figure 22. The ^{1}H-NMR spectrum of V-DNP in DMSO-d_6.

2.2.3 Synthesis of V-COOH

The synthesis of V-COOH is shown in Figure 23. The 60% ethanol was used as a solvent in all syntheses. Et_3N was added to increase pH and diminish protonation of the second pyridine ring with a free electron pair. The procedure proceeded for 1 hour and was checked with TLC, using Hx: EtAc=1.0:1.0 and pure methanol system until the full conversion of V-DNP. After the end of the reaction, the solution was evaporated, the precipitate was dissolved in a small amount of ethanol, and then EtAc was added to precipitate V-COOH. The solution was centrifuged at 6000 rpm for 10 minutes, and then the solvent was removed. Precipitate was washed three times with EtAc and then dried at room temperature under vacuum. 4. The experiments for optimization of V-COOH synthesis are summarized in Table 4. The purification of V-COOH is complicated because of the coprecipitation of V-COOH with PABA, probably because of protonation of a residual fraction of PABA after the removal of solvents and Et_3N. The ^{1}H-NMR spectrum of pure V-COOH is shown in Figure 24.

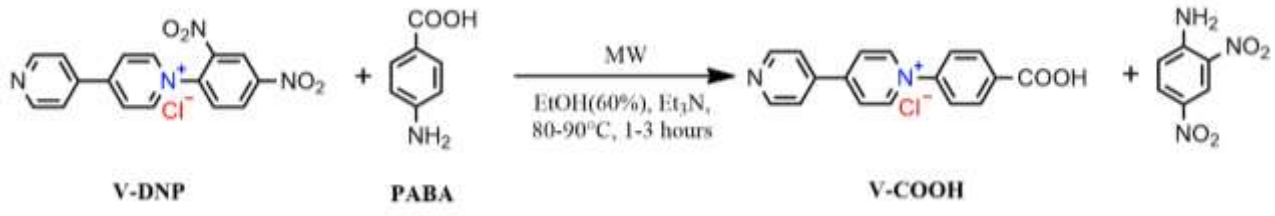

Figure 23. The synthesis of V-COOH.

Table 4. The optimization protocols for the synthesis of V-COOH

№	Mass of V-DNP (mg)	Mass of PABA (mg)	Ratio of eq.	Vol. (mL)	Et_3N (μL)	Temp. (°C)	Time (hours)	Product mass (mg)	Yield (%)
1	106	83	1.0:2.0	3	-	80	3	42	35
2	107	83	1.0:2.0	3	73	80	1	40	43
3	201	191	1.0:2.5	3	194	80	2	99.3	43
4	210	143	1.0:2.0	3	118	80	1	88.03	51
5	200	160	1.0:2.1	6	165	80	1	88.3	39
6	500	210	1.0:1.1	6	213	90	1	216	38

The V-COOH has bad solubility in MeCN, acetone, EtAc, and lower solubility in EtOH compared to V-DNP. ^{1}H-NMR (600 MHz, DMSO-d_6) of V-COOH is shown in Figure 24: δ

9.52 (d, *J* = 6.4 Hz, 2H), 8.91 (d, *J* = 5.0 Hz, 2H), 8.78 (d, *J* = 6.3 Hz, 2H), 8.16 (d, *J* = 5.0 Hz, 2H), 8.11 (d, *J* = 8.0 Hz, 2H), 7.80 (d, *J* = 8.0 Hz, 2H). Yield 50%.

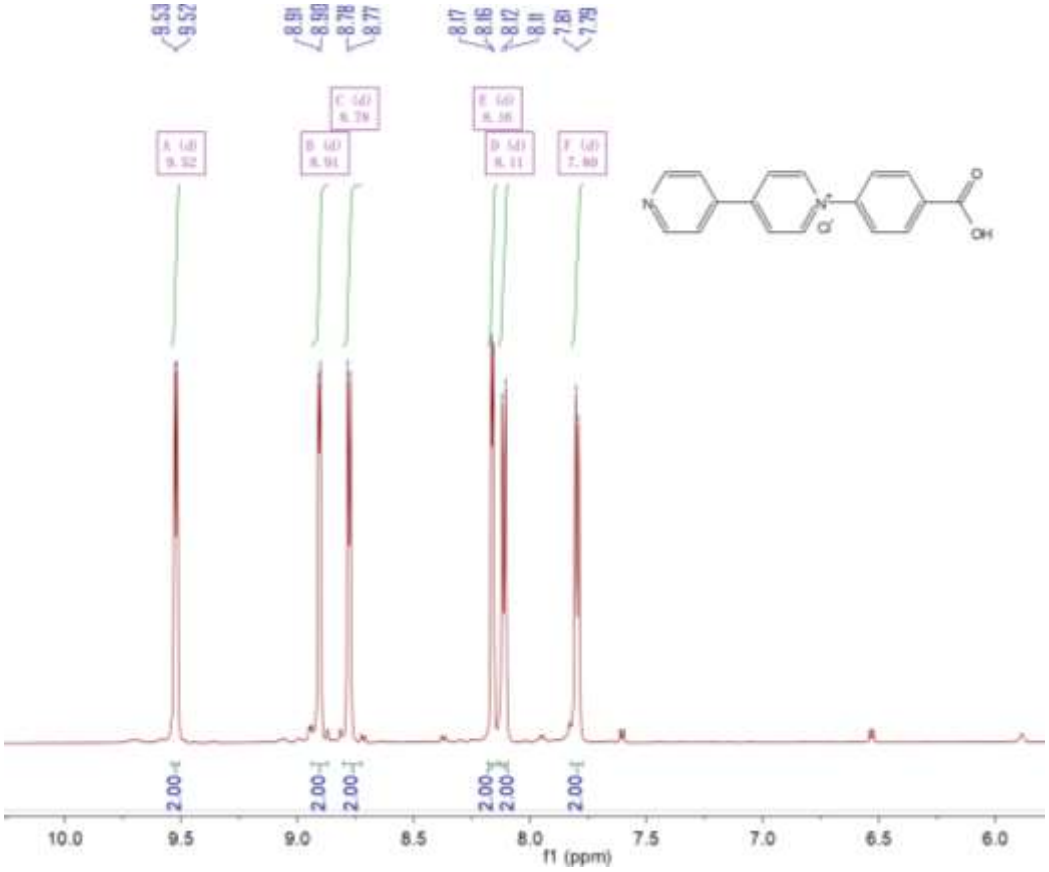

Figure 24. The ^{1}H-NMR spectrum of V-COOH in DMSO-d_6.

2.2.4 Synthesis of V-OH

The synthesis of V-OH is shown in Figure 25. Generally, 60% ethanol was used as a solvent in all syntheses. Et_3N was added to increase pH and diminish protonation of the second pyridine ring with a free electron pair. The procedure proceeded for 1 hour and was checked with TLC, using Hx: EtAc=1.0:1.0 and pure methanol system until the complete conversion of V-DNP. After the end of the reaction, the solution was evaporated, the precipitate was dissolved in a small amount of ethanol, and then EtAc was added to precipitate V-COOH. The solution was centrifuged at 6000 rpm for 10 minutes, and the solvent was removed. Precipitate was washed three times with EtAc and then dried at room temperature under vacuum.

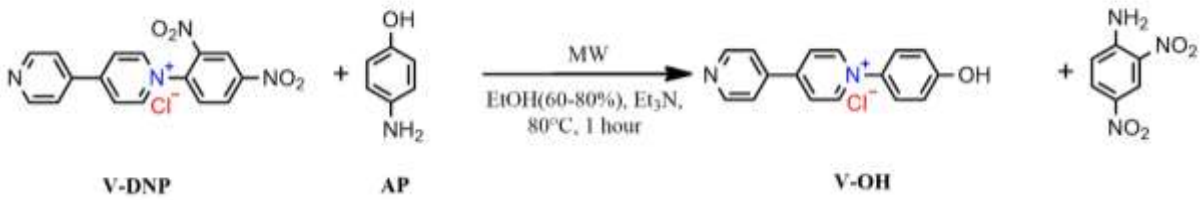

Figure 25. The synthesis of V-OH.

The first three syntheses were unsuccessful due to the formation of hard-to-separate by-products and the coprecipitation of AP with viologen. However, the addition of Et_3N allowed for the maximization of conversion. Et_3N increases pH, diminishing protonation of the second pyridine ring with a free electron pair. The experiments for optimizing V-OH synthesis are summarized in Table 5. Similar to V-COOH, the purification is complicated because of the coprecipitation of V-OH with AP. The NMR spectrum of pure V-OH is shown in Figure 26.

^{1}H-NMR (600 MHz, DMSO-d_6) of V-OH: δ 10.62 (s, 1H), 9.42 (d, J = 6.9 Hz, 2H), 8.90 (d, J = 6.1 Hz, 2H), 8.74 (d, J = 6.3 Hz, 2H), 8.14 (d, J = 6.0 Hz, 2H), 7.74 (d, J = 7.7 Hz, 2H), 7.10 (d, J = 7.2 Hz, 2H). Yield 48%.

Table 5. The optimization protocols for the synthesis of V-OH.

№	Mass of V-DNP (mg)	Mass of AP (mg)	Ratio of eq.	Solvent (mL)	Et_3N (μL)	Temp. (°C)	Time (hours)	Prod. (mg)	Yield (%)
1	104	66	1.0:2.0	3 mL of EtOH (80%)	-	100	1	97	- (not isolated)
2	108	67	1.0:2.0	3 mL of EtOH (60%)	-	80	1	96	- (hard to purify)
3	108	82	1.0:2.5	3 mL of EtOH (60%)	-	80	1	88	- (hard to purify)
4	200	151	1.0:2.5	3 mL of EtOH (60%)	77.6	80	1.5	83	52%
5	94	63	1.0:2.2	3 mL of EtOH (60%)	80	80	1.5	58	73%

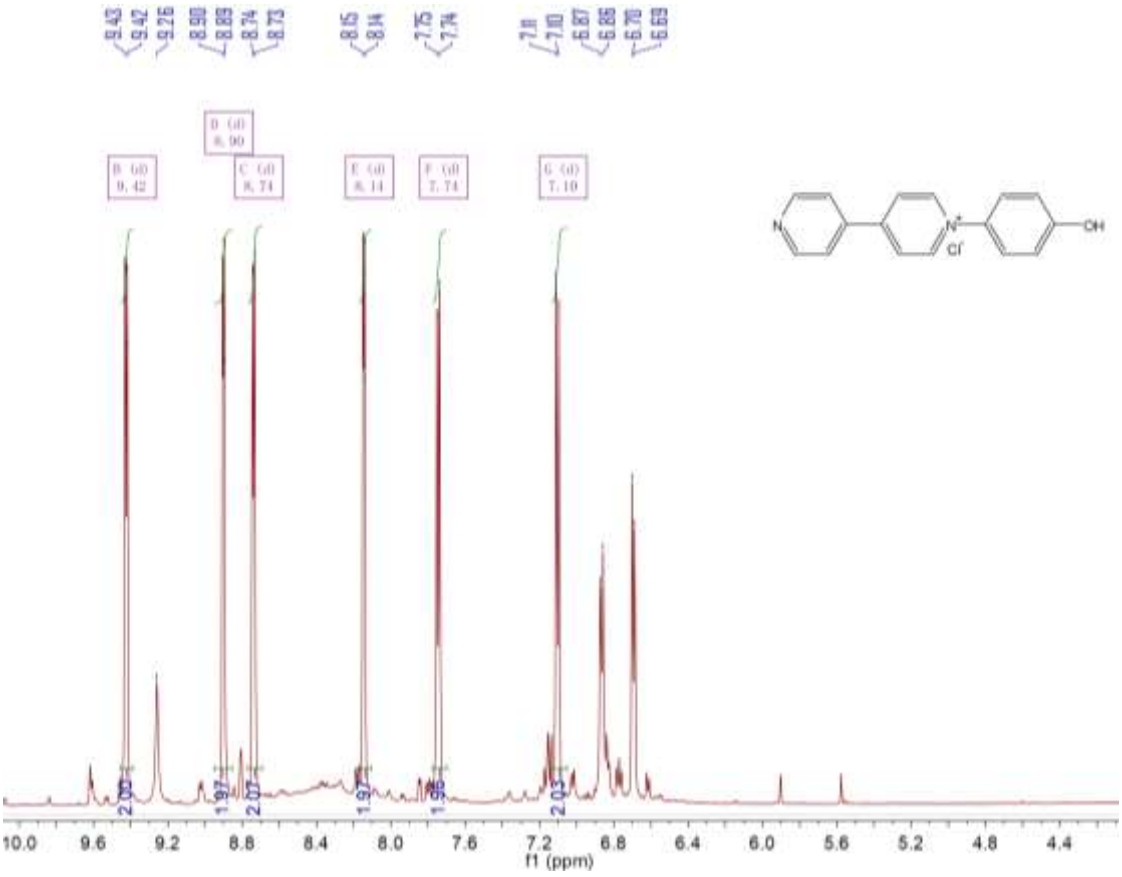

Figure 26. The ^{1}H-NMR spectrum of V-OH in DMSO-d_6.

2.2.5 Synthesis of Bn-V-COOH and Me-V-COOH

A huge (30 eq.) excess of methyl iodide was used to attach the methyl group to DMF. After the reaction, the product was precipitated from the solution with $CHCl_3$ and then centrifuged. 15 mg of solid was obtained, but the NMR spectrum showed the formation of another product, probably the methyl ester of Me-V-COOH (Figure 27).

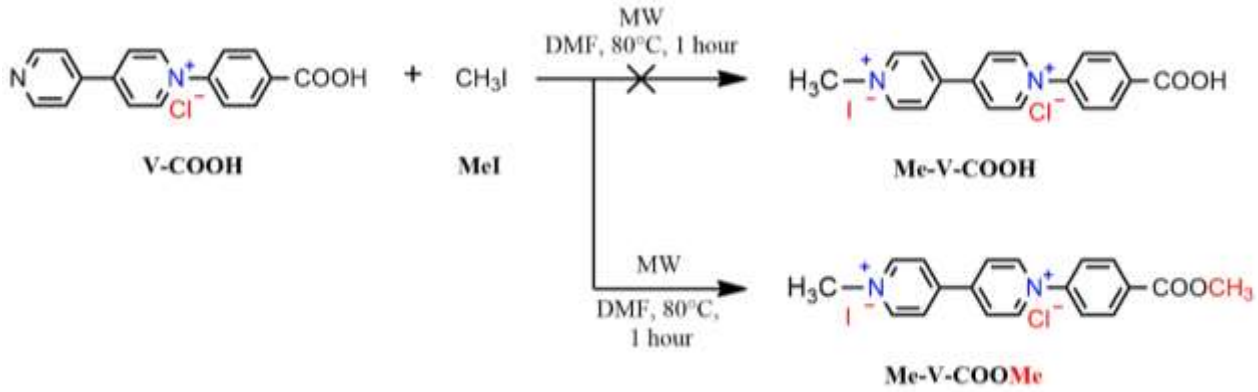

Figure 27. The synthesis of Me-V-COOH. The formation of methyl ester.

The 15 mg of solid was obtained, but the NMR spectrum showed formation of another product, probably the methyl ester of Me-V-COOH (Figure 23). The **^{1}H-NMR** (500 MHz, DMSO-d_6) of Me-V-COOH is shown in Figure 28: δ 9.73 (d, J = 6.6 Hz, 2H), 9.34 (d, J = 6.3 Hz, 2H), 8.99 (d, J = 6.6 Hz, 2H), 8.33 (d, J = 8.7 Hz, 2H), 8.12 (d, J = 8.6 Hz, 2H), 4.47 (s, 3H), 3.95 (s, 3H). Peak at 3.95 is a methyl group next to oxygen, formed by methylation of carboxylic acid by CH_3I. Peak at 4.47 is a methyl group next to the nitrogen of the second pyridine ring.

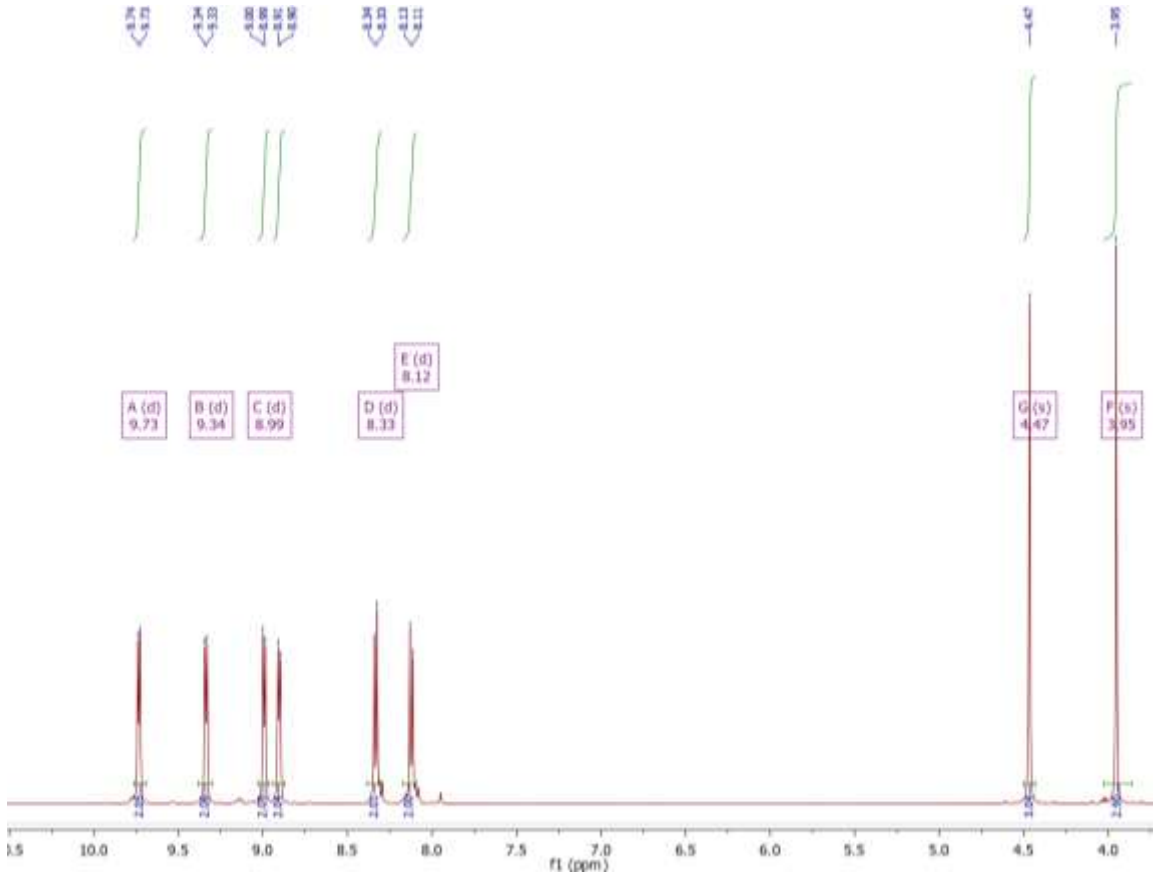

Figure 28. The ^{1}H-NMR spectrum of the product of the methylation of V-COOH in DMSO-d_6. According to the spectrum, the possible structure of the product is Me-V-COOMe.

It should be noted that the anions could be exchanged during the reaction, and the produced viologens could have a different anion composition than that we assumed.

The benzyl group was attached using an excess (3 eq.) of benzyl bromide (BnBr) in DMF to avoid hydrolysis of BnBr (Figure 29). After the reaction, the product was precipitated from the solution with an excess of EtAc and $CHCl_3$ and then centrifuged at 6000 rpm for 10 minutes. After removing the solvent, the product was washed 3 times with EtAc and dried at room temperature.

Figure 29. The synthesis of Bn-V-COOH.

The **^{1}H-NMR** of Bn-V-COOH is shown in Figure 30. **^{1}H-NMR** (500 MHz, DMSO-d_6): δ 13.62 (s, 1H), 9.73 (d, J = 5.8 Hz, 2H), 9.64 (d, J = 5.5 Hz, 2H), 8.96 (dd, J = 13.0, 5.8 Hz, 4H), 8.29 (d, J = 8.2 Hz, 2H), 8.10 (d, J = 8.1 Hz, 2H), 7.69 (d, J = 7.2 Hz, 2H), 7.48 (d, J = 7.5 Hz, 3H), 6.02 (s, 2H).

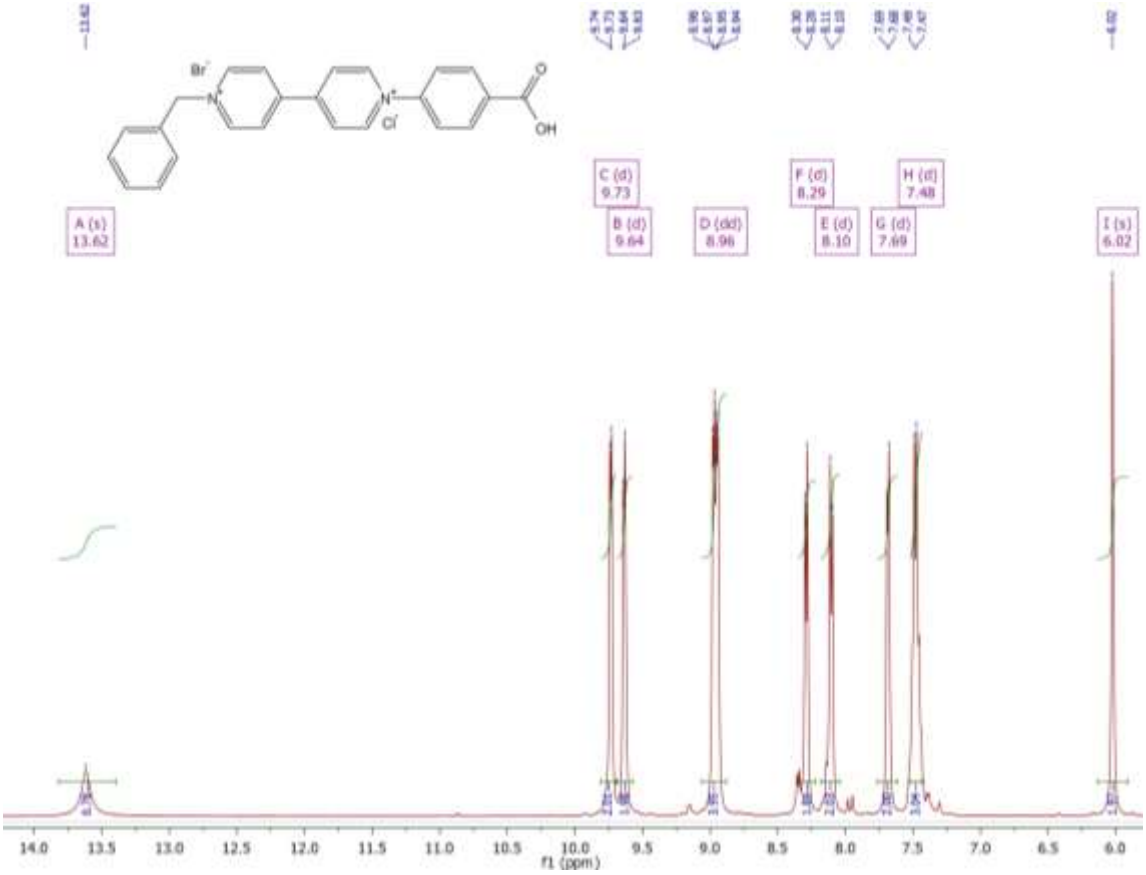

Figure 30. The ^{1}H-NMR spectrum of Bn-V-COOH in DMSO-d_6.

2.3 The fabrication of the electrochromic device

The electrochromic device was assembled according to procedures made by Choi et al (simple ITO or ITO-PET plates) [12] or Qian et. al 2024 (electrodes modified by TiO_2) [17].

The FTO (Fluorine-doped Tin Oxide) glass was used for both electrodes, providing a conducting layer and serving as a base for the upper layers**.** The mesoporous TiO_2 layer was chosen to work in tandem with carboxyphenylated viologens to provide an anchoring side for carboxylic groups, enhancing the adhesion of viologens to the cathode and improving response time [1]. Additionally, TiO_2 film prevents direct contact between the FTO surface and electrolyte, resulting in a lower recombination effect [2]. The bare FTO glass was chosen as an anodic material to preserve the transparency of the electrochromic device; instead, the redox complementary agent was added in an electrolyte solution in equimolar amounts to close the redox cycle. Ferrocene (Fc) was chosen as a redox complementary agent because it decreases the response time [3,7]. An example of the tandem work of viologen and ferrocene is shown in Figure 31.

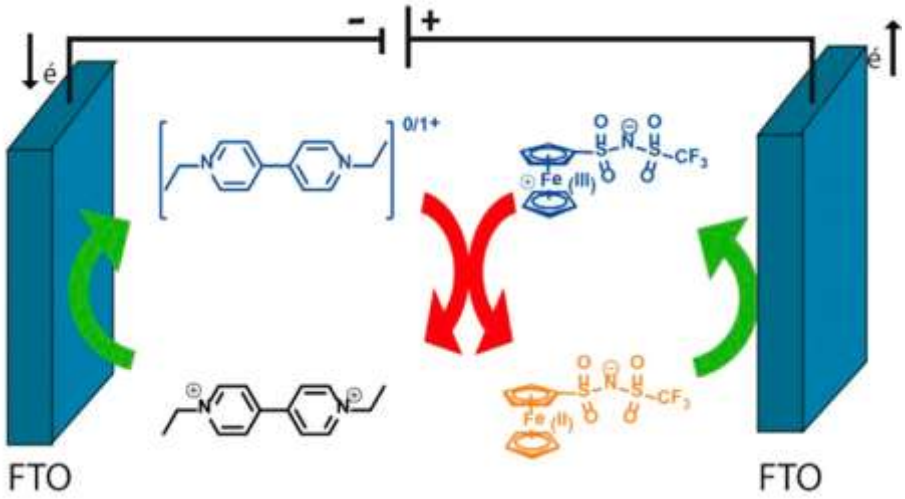

Figure 31. The mechanism of viologen and ferrocene-derivative tandem work. Adapted with permission from ref. 21. Copyright 2017 American Chemical Society.

The cathode part was prepared according to the following procedure: the FTO substrates were preliminarily cleaned with soap, distilled water, and ethanol, sonicated in ethanol solution for 15 minutes, then dried in a drying oven. The TiO_2 film was applied in two stages: a compact layer and a transparent layer. The compact layer solution was prepared by dissolving 1542 microliters of titanium tetraisopropoxide (TTIP) in 30 mL of 2 M HCl solution. After dissolving, 70 mL of distilled water was added. The FTO substrates were immersed in the solution and put at 70°C for 30 minutes. Next, the substrate was rinsed with distilled water and sintered in an oven at 500 °C for 30 minutes. The second, transparent layer was made by application of transparent titania paste using the doctor blade method on the circular area.

The substrate was dried for 30 minutes in air, then sintered in the oven (125°C – 5 minutes, 325°C – 10 minutes, 425°C – 15 minutes, 500 °C – 30 minutes). The prepared FTO/TiO_2 glasses are shown in Figure 32.

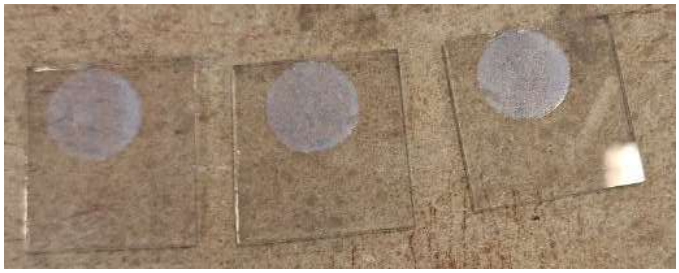

Figure 32. The obtained FTO/TiO_2.

Two different approaches have been suggested and tested: pre-anchoring and electrochromic gel.

Pre-anchoring approach – viologen is pre-anchored before the addition of electrolyte. The FTO/TiO_2 substrate was immersed in 15 mL of 0.2 M solution of monosubstituted viologen containing one carboxyphenyl group ([1-(4-carboxyphenyl)-(4,4′-bipyridinium)] chloride; V-COOH). After 12 hours, the substrate was removed from the solution, gently washed with ethanol, and dried at 70°C. After drying, the electrolyte gel (gel composition: PC:PMMA=9:1, 0.1 M $LiClO_4$, 0.01 M Fc) was applied on the cathode and sandwiched with bare FTO anode.

The observation showed the visible color change of TiO_2 paste after 1 hour (Figure 33), indicating the good absorption of viologen on TiO_2.

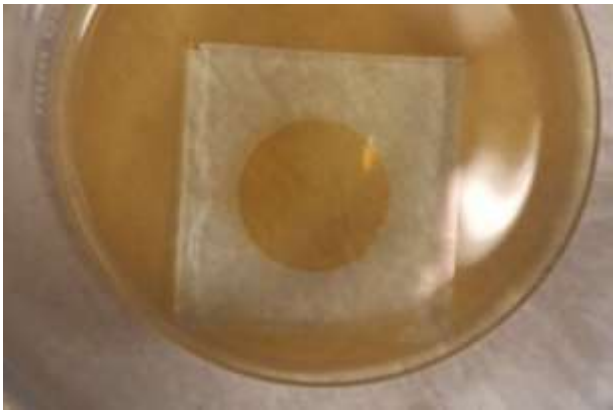

Figure 33. The FTO/TiO_2 substrate in the viologen solution.

Mixed approach – viologen is mixed with an electrolyte and applied to one layer. The 0.01 M of the same monosubstituted viologen (V-COOH) was dissolved in gel with the same composition (PC: PMMA=9:1 by weight, 0.1 M $LiClO_4$, 0.01 M Fc), sonicated, and stirred

until complete dissolution of viologen. The electrochromic gel was applied on the surface of the FTO/TiO_2 substrate and sandwiched with a bare FTO anode. Both assembled devices were tested using the chronoamperometry method at -0.8 V with a current range of 1 mV, then bleached at 0 V.

2.4 Cyclic voltammetry

Cyclic voltammetry (CV) was recorded with a 0.01M V-COOH using a PalmSense4 potentiostat. The electrochrome was pre-dropped on a glassy carbon electrode (GCE), and cyclic voltammetry was recorded in MeCN 0.1M $LiClO_4$, 0.1 mM LiI/I_2 system.

2.5 Optical measurements

For analysis of optical properties, 0.001 M of electrochrome (V-COOH, V-OH, Me-V-COOH, Bn-V-COOH), mixed with 0.0012 M of Fc, 0.1 M of (Lithium bis(trifluoromethanesulfonyl)imide) LiTFSI were mixed in 1 mL of PMMA:PC (weight ratio PMMA:PC =1:6). Obtained gel solutions were sandwiched between two indium-tin oxide-coated glasses (ITO). Transmission spectra were recorded for bleached and colored (at -1.2V) states using an Avantes ULS2048CL-EVO UV-Vis spectrometer and an Avantes AvaLight-DHc light source.

Optical modulation (ΔT) is the primary parameter [2] for demonstrating the color-switching ability of an EC material/device. It is defined as the difference in transmittance between colored and bleached states:

$$\Delta T = T_{bleached} - T_{colored}$$

Contrast ratio (CR) is another widely accepted [2] performance index for evaluating the color-switching ability, as shown below:

$$CR = T_{bleached}/T_{colored}$$

The optical modulation was calculated individually for each viologen based on the wavelength with maximal transmission in the colored state.

2.6 Safety considerations

Viologen toxicity: potentially, all viologens are toxic and lethal to humans. The methyl viologen or paraquat, the most famous member of the viologen family, was a widely used herbicide, earning a bad reputation for its illegal application in murder and suicide [21]. The toxicity of all viologen derivatives is linked to the catalytic function of $MV^{+\bullet}$ in the oxygen reduction reaction with the formation of superoxide (O_2^-) species [8].

3. RESULTS AND DISCUSSION

3.1 Synthesis discussion

The attachment of aryl moieties in the first position to viologens is problematic due to the nucleophilicity of both species, the nitrogen of bipyridine, and the aryl rings. The Zincke salts are used as intermediate compounds for those transformations because of the strong electron-withdrawing effect of the two nitro groups. During the synthesis procedure, it was empirically found that the attachment of DNCB proceeds relatively easily, with the formation of some amount of di-substituted DNP-V-DNP Zincke salt. However, the attachment of DNCB to phenylated viologen is more challenging and not readily achievable at 80-100°C (Figure 34).

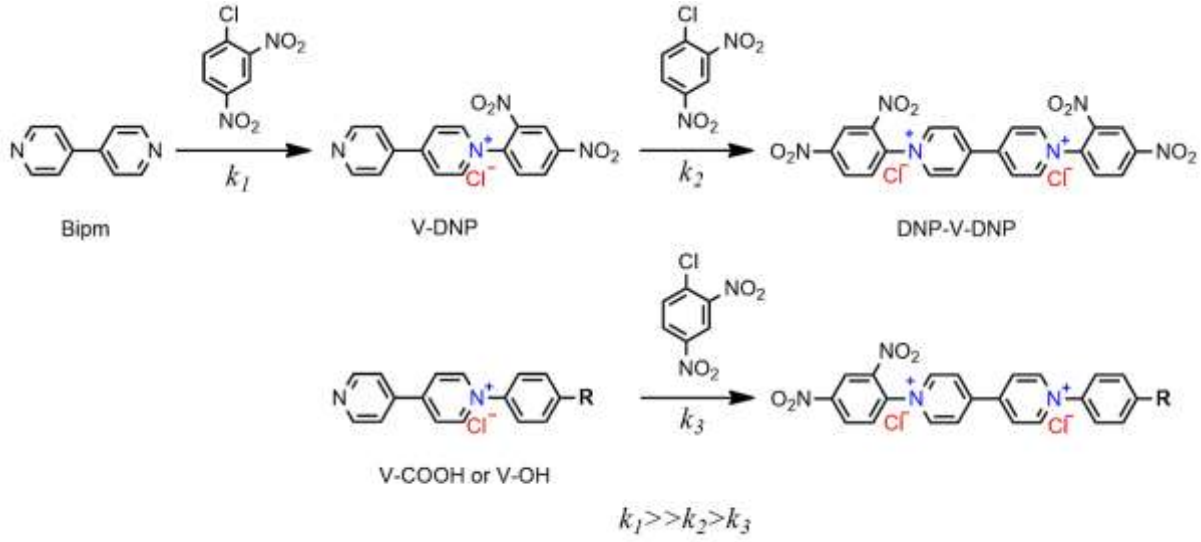

Figure 34. The comparison of DNCB addition kinetics.

Looking back on the reaction mechanism of the Zincke reaction, two critical steps could be distinguished: nucleophilic aromatic substitution (*SnAr*) and nucleophilic addition to the Zincke salt (*AN*). The extent of electronic deficiency of pyridine has a different effect on the kinetics of these two reactions: EWGs decrease the reactivity of pyridine to react with DNCB, while EWGs also facilitate aryl addition (Figure 35).

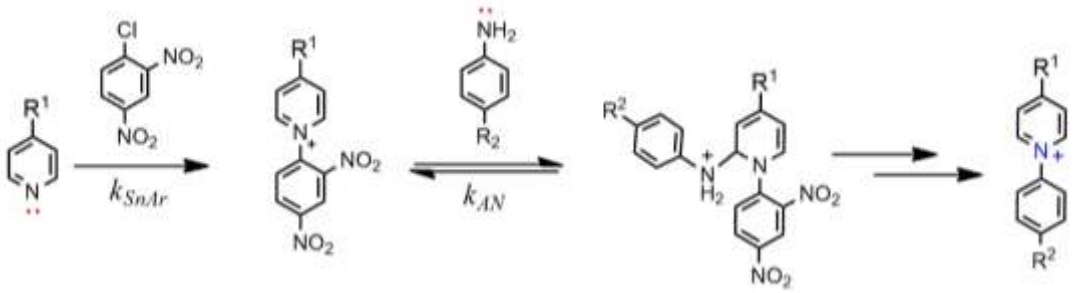

Figure 35. The major steps in the Zincke reaction.

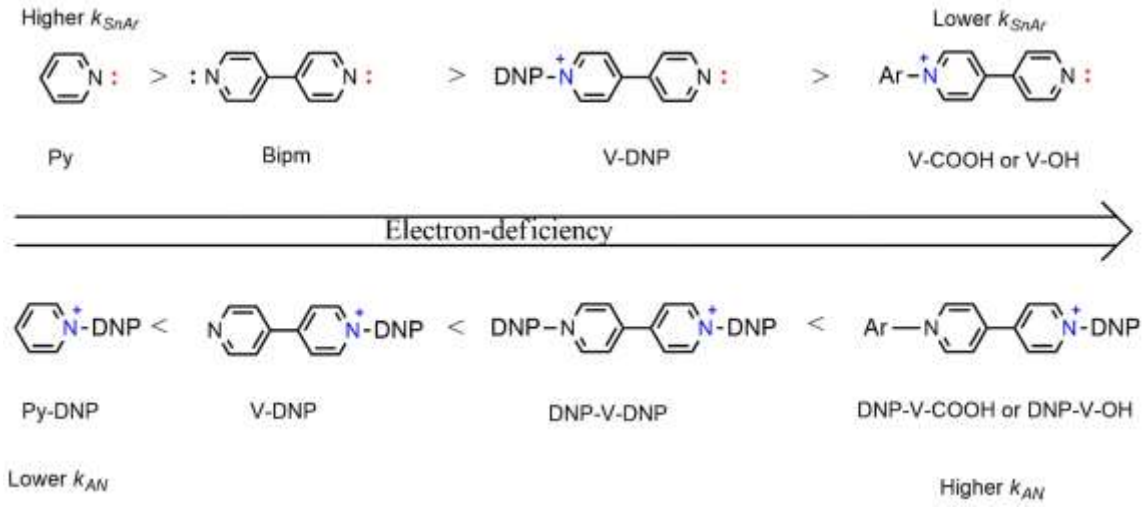

Figure 36. The effect of substituents on electron deficiency and reactivity of pyridine/bipyridine derivatives.

The treatment of monosubstituted arylated products is complicated by the co-precipitation of mono-arylated viologen and aniline derivative (PABA and AP), probably due to the protonation of the second pyridine ring with protons of these species, consequent complexation, and co-crystallization.

With the growth of electron deficiency, the rate of addition of DNCB (k_{SnAr}) decreases (pyridine ring becomes less nucleophilic) while it increases the rate of nucleophile addition (k_{NA}). On the one hand, it is beneficial for reaction with aniline, but at the same time, it could make viologen more vulnerable to nucleophiles in the reaction system (EtOH, H_2O, Et_3N) and consequently less stable. To conclude, the electron deficiency slows down the rate of the first step of the Zincke reaction but accelerates the second step.

3.2 Electrochemical experiments

Both approaches showed color changes on the site where transparent TiO_2 had been applied (Figure 37). In both cases, small bubbles appeared inside the device, which was due to electrolyte leakage. Due to electrolyte loss, the devices lost their ability to change color in parts where electrolytes disappeared.

Different suggestions have been tested to optimize the work of ECDs. First, the ratio of PMMA to PC was increased up to 15%, in order to increase viscosity and gelify the solution more. Second, the electrolyte was changed from $LiClO_4$ to TBAP, in an attempt to avoid the formation of bubbles.

The preparation of electrochromic gel is more optimal because of better control of the amount of electrochrome in the device, ensuring an equivalent ratio of electrochrome and redox complementary agent in the system, which is essential to maintain the long-term sustainability of the process.

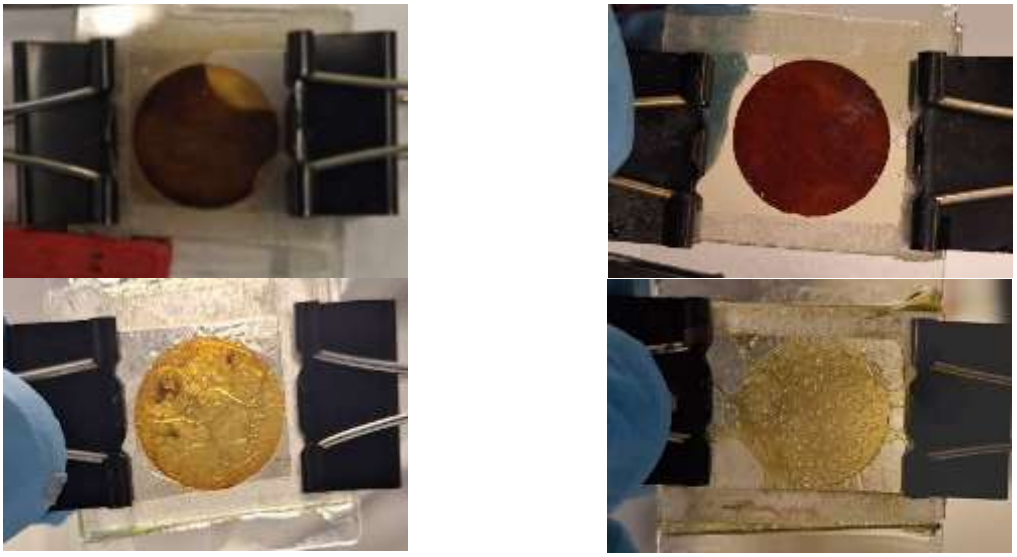

Figure 37. The comparison of two approaches: pre-anchored (left) and a mixed (right).

The formation of bubbles inside occurs during the electrochemical experiment, which could be a sign of electrolysis. The leaking of ECD with 10% PMMA. The increase of PMMA content up to 15% has a little improvement in electrolyte, despite the leakage occurring again. The rise of PMMA increases the viscosity of the electrolyte, which, on one hand, decreases the possibility of leakage, but also reduces the mobility of ions inside the ECDs, which would negatively affect ECDs' performance, particularly on the response speed (coloration and bleaching). Nevertheless, the instability of ECD led to an inability to fully and adequately

investigate the electrochromic performance of ECDs. It was observed that the coloration of ECD took less than 2 seconds, while bleaching required more time (approximately 15 seconds), but the record of response speed requires a more formal approach (Figure 38).

State	Initial state	Colored (-1.2V)	Bleaching by switching voltages (+1.2V)
ECDs	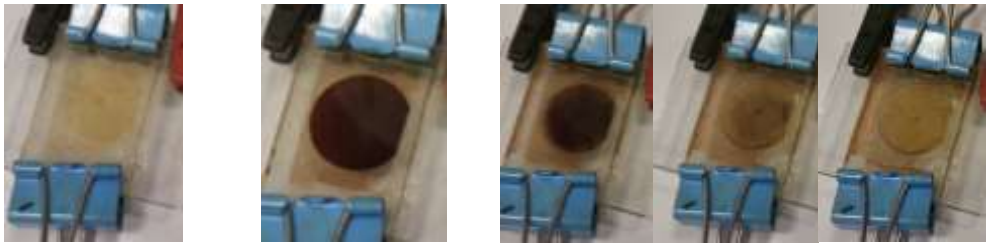		

Figure 38. Visual observations on ECD reversible coloration.

The ECDs failed after a few runs are mainly related to the design of ECDs and electrolyte composition. Another ECD based on V-COOH was made and used to analyze color change at different voltages (Figure 39). Despite similar composition, the ECDs showed green coloration on the surface of the TiO_2 circle at voltages lower than -0.6V and magenta in free volume, at voltages lower than -1.0V. The possible reason is the different amount of impurities, particularly residual PABA. The ECD presented in Figure 39 contained more PABA (approximately 4:1), compared to one used before (Figure 38), which could protonate V-COOH, providing better coloration. Another explanation is that the second ECD was less concentrated, again, due to the impurities (PABA, water).

V	-0.2	-0.4	-0.6	-0.8	-1.0	-1.4	-1.6
ECDs							

Figure 39. Visual observations on ECD at different voltages.

CV of V-COOH shown in Figure 40. The approximate reduction potentials are -0.23V and -0.52V for $MV^{2+} \rightarrow MV^{+\bullet}$ and $MV^{+\bullet} \rightarrow MV^{0}$, respectively.

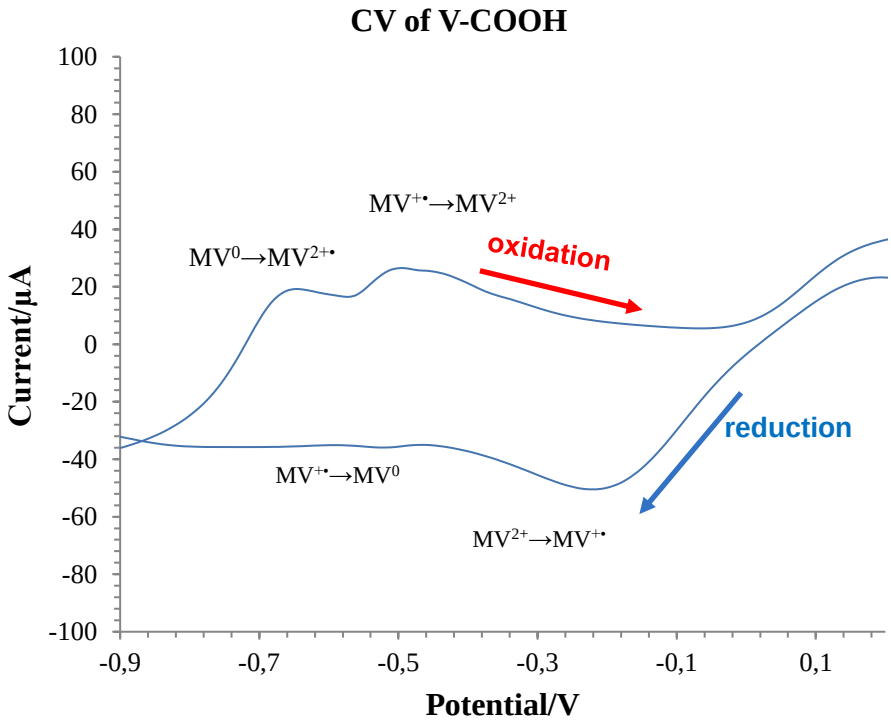

Figure 40. The CV of V-COOH on GCE in MeCN 0.1M $LiClO_4$, 0.1 mM LiI/I_2 system scanned at 100 mV/s.

3.3 Transmittance contrast

The transmission spectra are presented in Figures 41-44; The optical modulation values were calculated and summarized in Table 6. Images of four assembled cells containing 0.001M of electrochrome (V-COOH, V-OH, Me-V-COOH, Bn-V-COOH) before and after coloration (-1.2V) are shown in Figure 41. Viologens without a second substituent (V-COOH, V-OH) showed worse optical modulation (lower ΔT, CR) than those that have a substituent (Me-V-COOH, Bn-V-COOH).

Table 6. The optical properties of assembled devices.

Compound	$\lambda_{max.}$(nm)	$T_{max.}$ (colored)	ΔT (%)	CR
V-COOH	771	48.33%	25.13	1.52
V-OH	720	64.77%	23.47	1.36
Me-V-COOH	693	40.91%	41.44	2.01
Bn-V-COOH	768	26.22%	33.09	2.26

V	V-COOH	V-OH	Me-V-COOH	Bn-V-COOH
0				
-1.2				

Figure 41. ECDs before and after coloration.

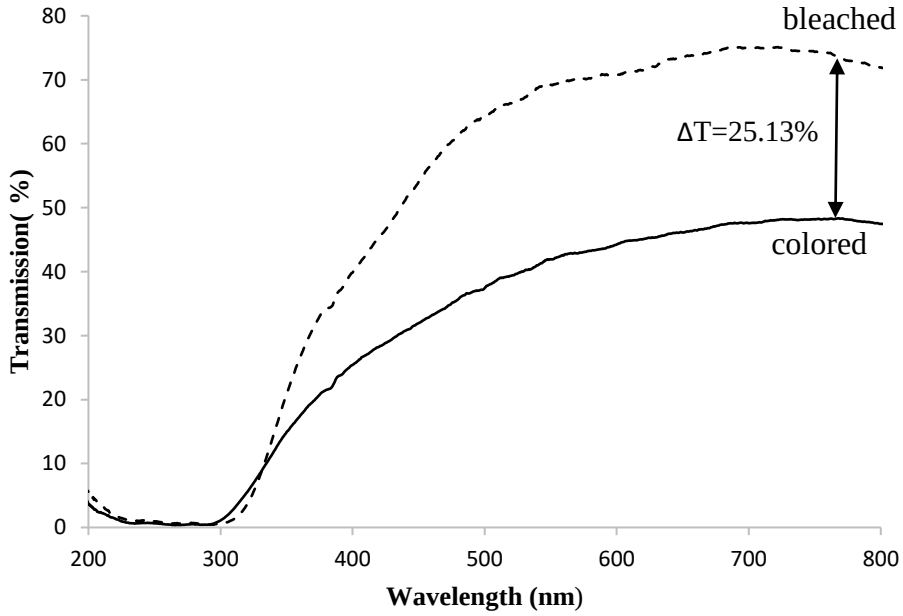

Figure 42. The transmission diagram of V-COOH.

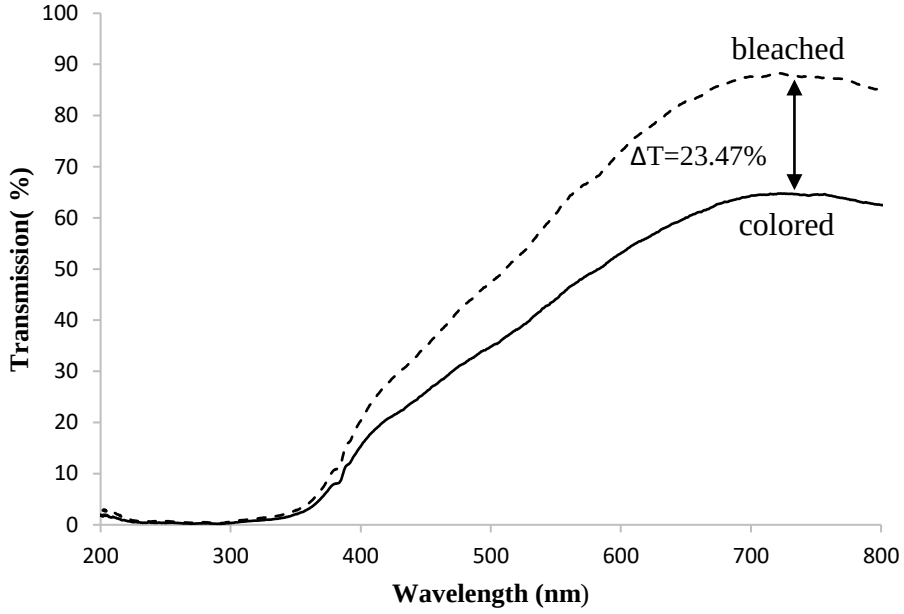

Figure 43. The transmission diagram of V-OH.

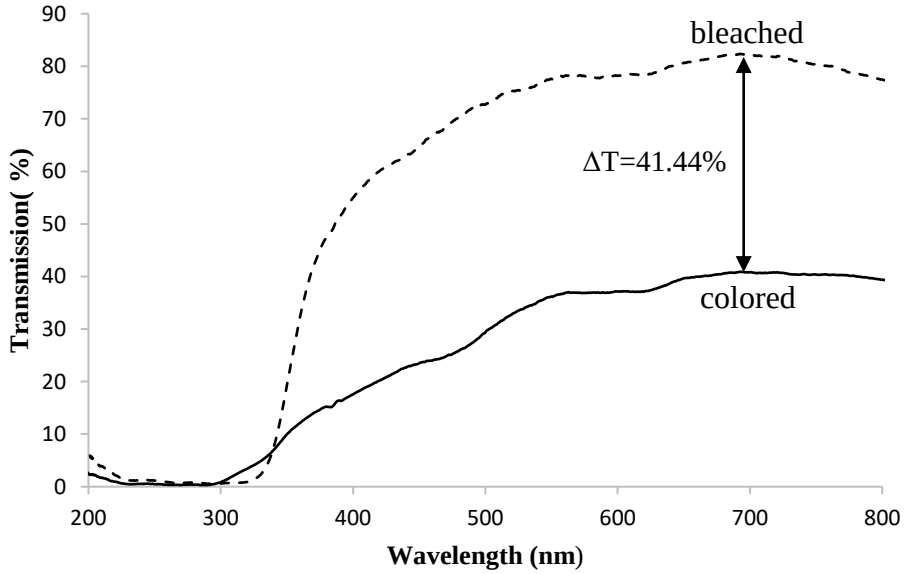

Figure 44. The transmission diagram of Me-V-COOH.

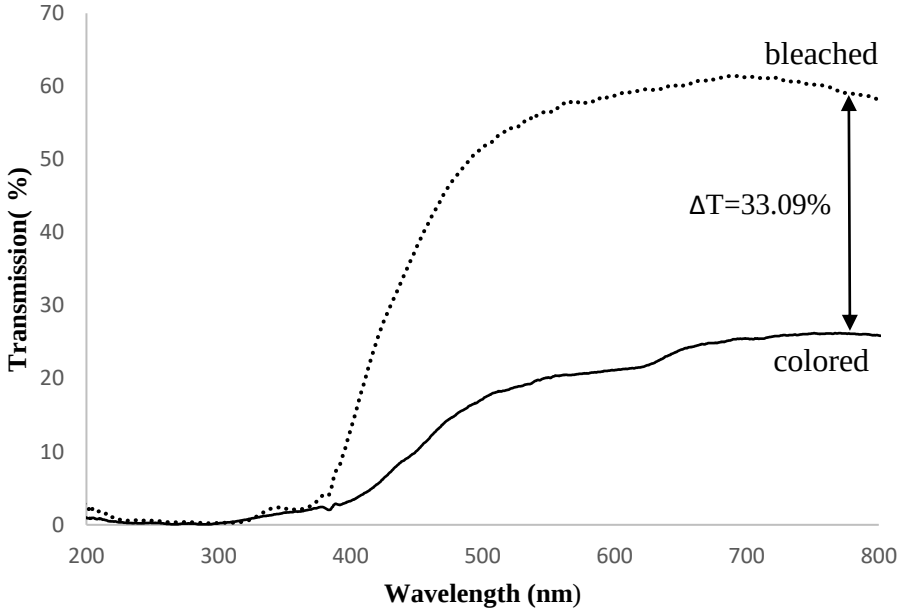

Figure 45. The transmission diagram of Bn-V-COOH.

Possible reason is that the mono-substituted viologen cannot form a colorful state on the structural level: while disubstituted viologens can form a cation-radical state ($MV^{+\bullet}$, which is the main colorful form [7]), the monosubstituted viologens form radical (MV•), which is less optically active form than the cation-radical (Figure 46). The existing ability of the synthesized mono-substituted viologens (V-COOH, V-OH) can be related to the presence of impurities, initial reagents (PABA, AP), which could protonate bipyridine and form protonated disubstituted salts. The pure compounds showed even less electro-optical activity than those containing some (20-50%) fraction of the initial reagents. This hypothesis also explains the presence of PABA and AP on initial NMR spectra and problematic purification due to the formation of protonated viologens, as shown in Figure 47.

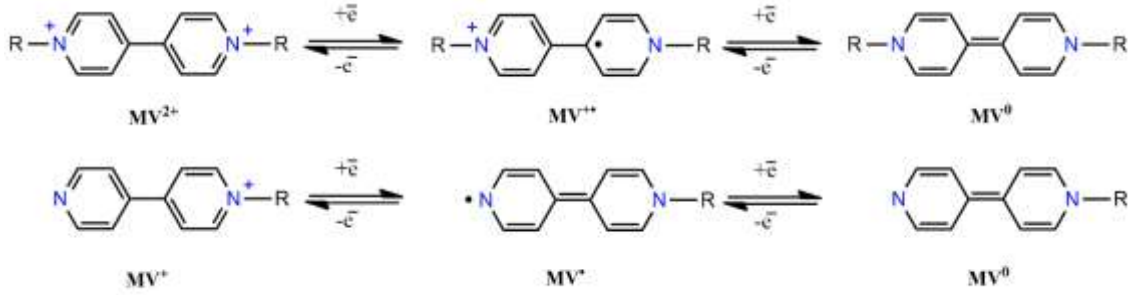

Figure 46. The difference between the states of disubstituted salt and monosubstituted viologens.

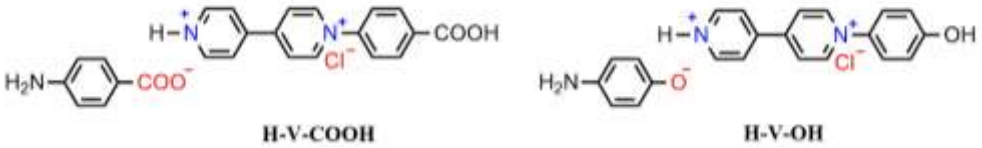

Figure 47. The protonated H-V-COOH and H-V-OH

4. CONCLUSIONS AND FUTURE WORK

Four asymmetric viologens, V-COOH, V-OH, Bn-V-COOH, and Me-V-COOMe were synthesized and used to fabricate ECDs. Their bleached and colored states were characterized using UV-Vis spectroscopy. The viologens with a second substituent showed better optical performance: Bn-V-COOH showed the lowest $T_{max.}$ of colored state (26.22%), higher CR (2.26), while Me-V-COOH showed the highest ΔT (41.44%). The viologens without the second substituent showed significantly lower T_{max}, ΔT, and CR; V-COOH showed slightly higher results than V-OH. Therefore, the absence of the second substituent critically deteriorates the electrochromic properties of viologen.

While the current work's outcomes are modest, further investigation could provide a more comprehensive review of the performance of ECD with asymmetric viologen.

–Optimize the composition of electrolyte gel to achieve adequate coloration, avoid leaking, and ensure good ion mobility. The current design and fabrication procedure require optimization, due to the instability of ECD after few runs, mainly due to the leakage and formation of bubbles. The appropriately assembled ECDs are required for further electrochemical experiments.

–Make more experiments to analyze the performance of ECDs: (i) find an appropriate system and record cyclic voltammetry at different scan rates to determine the potential for coloration reaction; (ii) record the rate of coloration/bleaching of ECDs; (iii) investigate the stability of ECDs after multiple cycles.

–Compare the performance of asymmetric viologens with symmetric analogues.

–Synthesize asymmetric viologens with other functional groups, particularly with other aryl moieties.

REFERENCES

1. Stolar, M. Organic electrochromic molecules: Synthesis, properties, applications and impact. *Pure Appl. Chem.* **2020**, *92*(5), 717–731. DOI:10.1515/pac-2018-1208

2. Gu, C.; Jia, A. B.; Zhang, Y. M.; Zhang, S. X. A. Emerging Electrochromic Materials and Devices for Future Displays. *Chem. Rev.;* **2022**, *122* (18), 14679–14721. DOI:10.1021/acs.chemrev.1c01055

3. Wu, W.; Guo, S.; Bian, J.; He, X.; Li, H.; Li, J. Viologen-based flexible electrochromic devices. *J Energy Chemistry*. **2024**, 93, 453–470. DOI:10.1016/j.jechem.2024.02.027

4. Ding, J.; Zheng, C.; Wang, L.; Lu, C.; Zhang, B.; Chen, Y.; Li, M.; Zhai, G.; Zhuang, X. Viologen-inspired functional materials: Synthetic strategies and applications. *J. Mater. Chem. A*, **2019**, *7*(41), 23337–23360. DOI:10.1039/c9ta01724k

5. He, X.; Chen, L.; Baumgartner, T. Modified Viologen- and Carbonylpyridinium-Based Electrodes for Organic Batteries. *ACS Appl. Mater. Interfaces*, **2023,** *16*(37), 48689-48705. DOI:10.1021/acsami.3c09856

6. Nuroldayeva, G.; Balanay, M. P. Flexing the Spectrum: Advancements and Prospects of Flexible Electrochromic Materials. *Polymers*, **2023**, 15 (13). DOI:10.3390/polym15132924

7. Monk, P.M.S.; Rosseinsky, D.V.; Mortimer R.J. in *Electrochromic Materials and Devices Based on Viologens*. Ed by Mortimer R.J.Ed.; Rosseinsky, D.V. Ed; Monk, P.M.S Ed.; Wiley, 2013, pp 57-90

8. Kathiresan, M.; Ambrose, B.; Angulakshmi, N.; Mathew, D. E.; Sujatha, D.; Stephan, A. M. Viologens: a versatile organic molecule for energy storage applications. *J.Mater. Chem.;***2021**, *9*(48),27215–27233. DOI:10.1039/d1ta07201c

9. Jhariat, P.; Warrier A.; Sasmal, A.; Das, S.; Sarfudeen, S.; Kumari, P.; Nayak, A.K.; Panda T. Reticular synthesis of two-dimensional ionic covalent organic networks as metal-free bifunctional electrocatalysts for oxygen reduction and evolution reactions. *Nanoscale*, **2024**, 16, 5665–5673. DOI:10.1039/D3NR05277J

10. Zeghbib, N.; Thelliere, P.; Rivard, M.; Martens, T. Microwaves and Aqueous Solvents Promote the Reaction of Poorly Nucleophilic Anilines with a Zincke Salt. *J. Org. Chem.;* **2016**, *81*(8), 3256–3262. DOI:10.1021/acs.joc.6b00208

11. Cheng, W. C.; Kurth, M. J. The Zincke reaction. A review. *Org. Prep. Proced. Int.* **2002**. *34*(6), 585–608. DOI:10.1080/00304940209355784

12. Choi, Y.; Kim, K. W.; In, Y. R.; Tang, X.; Kim, P.; Quy, V. H. V.; Kim, Y. M.; Lee, J.; Choi, C.; Jung, C.; Kim, S. H.; Moon, H. C.; Kim, J. K. Multicolor, dual-image, printed electrochromic displays based on tandem configuration. *Chem. Eng. J.;* **2022,** *429*, 132319. DOI:10.1016/j.cej.2021.132319

13. Leroy J. Kloeppner L.J.; Giri P.; Lin, R.; Theiste D.A. Electrochromic polyelectrolyte gel medium having improved creep resistance and associated electrochromic device. USA Patent US9500927B2, November 22, 2016.

14. Alesanco, Y.; Viñuales, A.;Cabañero, G.; Rodriguez, J.; Tena-Zaera, R.. *ACS Appl. Mat. In.* **2016**, 8 (43), 29619-29627. DOI: 10.1021/acsami.6b11321

15. Kim, M.; Kim, Y. M.; Moon, H. C. Asymmetric molecular modification of viologens for highly stable electrochromic devices. *RSC Adv.;* **2019**, 10, 394–401. DOI:10.1039/c9ra09007j

16. Feng, F.; Guo, S.; Ma, D.; Wang, J. An overview of electrochromic devices with electrolytes containing viologens. *Sol. Energy Mater. Sol. Cells.;* **2023**, *254*, 112270. DOI:10.1016/j.solmat.2023.112270

17. Qian, C.; Wang, P.; Guo, X.; Jiang, C.; Liu, P. High-contrast energy-efficient flexible electrochromic devices based on viologen derivatives and their application in smart windows and electrochromic displayers. *Sol. Energy Mater. Sol. Cells.;* **2024**, *266*, 112669. DOI:10.1016/j.solmat.2023.112669

18. Komoda, K.; Kawauchi, T. Size-controlled one-pot synthesis of viologen nanoparticles via a microwave heating technique. *Polym. J.*; **2021**. *53*(8), 937–942. DOI:10.1038/s41428-021-00480-4

19. Chen, Z.; Khoo, R.; Garzón-Ruiz, A.; Yang, C.; Anderson, C. L.; Navarro, A.; Zhang, X.; Zhang, J.; Lv, Y.; Liu, Y. . Quinoid-viologen conjugates: Redox properties and host-guest complex with cucurbiturils. *Mater. Today Chem.*, **2022**, *24*, 100933. DOI:10.1016/j.mtchem.2022.100933

20. Jhariat, P.; Panda, T. Recent advancement in viologen functionalized porous organic polymers (vPOPs) for energy and environmental remediation. *Mater. Adv.;* **2024**, *5*(10), 4055–4077. DOI:10.1039/d4ma00182f

21. Seetasang, S.; Kaneta, T. Portable two-color photometer based on paired light emitter detector diodes and its application to the determination of paraquat and diquat. *Microchem. J.* **2021**, *171*, 106777. DOI:10.1016/j.microc.2021.106777